การดูดซับกรดโอเลอิกโดยใช้ตัวดูดซับที่ได้จากกากอ้อย

นางสาววิมลมาศ ศิริวาณิชย์

วิทยานิพนธ์นี้เป็นส่วนหนึ่งของการศึกษาตามหลักสูตรปริญญาวิทยาศาสตรมหาบัณฑิต
สาขาวิชาเคมี
มหาวิทยาลัยเทคโนโลยีสุรนารี
ปีการศึกษา 2558

ADSORPTION OF OLEIC ACID USING ADSORBENTS DERIVED FROM SUGARCANE BAGASSE

Wimolmas Siriwanitch

A Thesis Submitted in Partial Fulfillment of the Requirements for the

Degree of Master of Science in Chemistry

Suranaree University of Technology

Academic Year 2015

ADSORPTION OF OLEIC ACID USING ADSORBENTS DERIVED FROM SUGARCANE BAGASSE

Suranaree University of Technology has approved this thesis submitted in partial fulfillment of the requirements for a Master's Degree.

Thesis Examining Committee

(Assoc. Prof. Dr. Jatuporn Wittayakun)
Chairperson

(Asst. Prof. Dr. Sanchai Prayoonpokarach)
Member (Thesis Advisor)

(Asst. Prof. Dr. Kunwadee Rangsriwatananon)
Member

(Asst. Prof. Dr. Rapee Utke)
Member

(Prof. Dr. Sukit Limpijumnong)
Vice Rector for Academic Affairs
and Innovation

(Prof. Dr. Santi Maensiri)
Dean of Institute of Science

วิมลมาศ ศิริวาณิชย์ : การดูดซับกรดโอเลอิกโดยใช้ตัวดูดซับที่ได้จากกากอ้อย (ADSORPTION OF OLEIC ACID USING ADSORBENTS DERIVED FROM SUGARCANE BAGASSE) อาจารย์ที่ปรึกษา : ผู้ช่วยศาสตราจารย์ ดร.สัญชัย ประยูรโภคราช, 61 หน้า.

กรดไขมันอิสระ (FFA) สามารถก่อให้เกิดปัญหาในกระบวนการผลิตไบโอดีเซล เช่น ทำให้เกิดการเสื่อมสภาพของตัวเร่งปฏิกิริยาและได้ไบโอดีเซลลดลง ดังนั้นการกำจัดกรดไขมันอิสระจากน้ำมันจึงมีความจำเป็นอย่างยิ่ง มีหลายวิธีในการลดปริมาณกรดไขมันอิสระออกจากน้ำมันและหนึ่งในนั้นคือการดูดซับ งานวิจัยนี้สนใจการแยกกรดไขมันอิสระออกจากน้ำมันโดยใช้ตัวดูดซับที่ทำได้จากชานอ้อยและเถ้าชานอ้อย ในการศึกษาใช้กรดโอเลอิกและกรดคาปริกเป็นตัวแทนของกรดไขมันอิสระ

ชานอ้อยนำมาปรับปรุงสมบัติด้วยกรดซัลฟิวริกแล้วนำไปเผา หรือนำไปเผาเพียงอย่างเดียวที่อุณหภูมิ 400 และ 500 °C ส่วนเถ้าชานอ้อยนำมาปรับปรุงสมบัติโดยแช่ในสารละลายโซเดียมไฮดรอกไซด์ด้วยระยะเวลาที่แตกต่างกัน หรือปรับปรุงสมบัติด้วยวิธีไฮโดรเทอร์มัล โดยแช่เถ้าชานอ้อยในสารละลายโซเดียมไฮดรอกไซด์ที่อุณหภูมิ 100 °C เป็นเวลา 72 ชั่วโมง ตัวดูดซับที่ได้นำมาใช้ในการดูดซับกรดโอเลอิก พบว่าเถ้าชานอ้อยที่ปรับปรุงสมบัติด้วยวิธีไฮโดรเทอร์มัลมีความจุการดูดซับสูงที่สุดคือ 40.2 มิลลิกรัมต่อกรัม เมื่อทำการทดลองการดูดซับโดยใช้ตัวดูดซับ 0.20 กรัมในสารละลายกรดโอเลอิกในไอโซออกเทน ความเข้มข้น 0.25% ที่อุณหภูมิ 25 °C เป็นเวลา 1 ชั่วโมง

เถ้าชานอ้อยที่ปรับปรุงสมบัติด้วยวิธีไฮโดรเทอร์มัลถูกนำมาศึกษาต่อในการดูดซับกรดโอเลอิกและกรดคาปริก พบว่าการดูดซับกรดโอเลอิกเป็นไปตามแบบจำลองไอโซเทอร์มของฟรุนลิช ส่วนการดูดซับกรดคาปริกเป็นไปตามแบบจำลองไอโซเทอร์มของแลงเมียร์

เมื่อนำเถ้าชานอ้อยที่ปรับปรุงสมบัติด้วยวิธีไฮโดรเทอร์มัลไปใช้ในการดูดซับกรดโอเลอิกและกรดคาปริกในน้ำมันถั่วเหลือง ความจุการดูดซับกรดโอเลอิกและกรดคาปริกที่ความเข้มข้นสารละลายกรด 0.50% มีค่า 11.6 มิลลิกรัมต่อกรัม และ 78.8 มิลลิกรัมต่อกรัม สำหรับที่ความเข้มข้นของสารละลายกรดเท่ากับ 1.00% ความจุการดูดซับกรดโอเลอิกและกรดคาปริกมีค่า 62.3

มิลลิกรัมต่อกรัม และ 90.3 มิลลิกรัมต่อกรัม ค่าการดูดซับที่ได้ในน้ำมันถั่วเหลืองมีค่าน้อยกว่าค่าการดูดซับที่ได้เมื่อทำการทดลองกับสารละลายกรดในไอโซออกเทน

สาขาวิชาเคมี ลายมือชื่อนักศึกษา____________________________

ปีการศึกษา 2558 ลายมือชื่ออาจารย์ที่ปรึกษา______________________

WIMOLMAS SIRIWANITCH : ADSORPTION OF OLEIC ACID USING
ADSORBENTS DERIVED FROM SUGARCANE BAGASSE.
THESIS ADVISOR : ASST. PROF. SANCHAI PRAYOONPOKARACH,
Ph.D. 61 PP.

FREE FATTY ACID, ADSORPTION, SUGARCANE BAGASSE, SUGARCANE BAGASSE ASH, OLEIC ACID, CAPRIC ACID

Free fatty acids (FFAs) can cause some problems in the production of biodiesel such as catalyst deactivation and lower biodiesel yield. Therefore, removal of FFAs from oil sources is of concern. There are many methods used for lowering FFA in oil and one of those is adsorption. In this work, sugarcane bagasse (SB) and sugarcane bagasse ash (SCBA) were investigated as adsorbents. Oleic and capric acid were used as representative of FFAs.

SB was treated with sulfuric acid and then calcined or calcined only at 400 and 500 °C. SCBA was treated in a solution of NaOH at various times or hydrothermally treated in a solution of NaOH at 100 °C for 72 h. The obtained adsorbents were used in the adsorption of oleic acid. It was found that hydrothermally treated SCBA had the highest adsorption capacity, 40.2 mg/g, when performing the adsorption experiment using 0.20 g adsorbent in a solution of 0.25% oleic acid in isooctane at 25 °C for 1 h.

Hydrothermally treated SCBA was investigated further for the adsorption of oleic and capric acid. The adsorption of oleic acid onto hydrothermally treated SCBA follows the Freundlich isotherm model, while the adsorption of capric acid onto the adsorbent follows the Langmuir isotherm model.

The application of hydrothermally treated SCBA on the adsorption of oleic and capric acid in soybean oil was made. The adsorption capacities for oleic acid and capric acid were 11.6 and 78.8 mg/g at the acid concentration of 0.50% and 62.3 and 90.3 mg/g at the acid concentration of 1.00%. The adsorption capacities were lower than those obtained in the solutions of isooctane.

School of Chemistry Student’s Signature________________________

Academic Year 2015 Advisor’s Signature________________________

ACKNOWLEDGEMENTS

First of all, I would like to thank my advisor Asst. Prof. Dr. Sanchai Prayoonpokarach, for giving me the opportunity throughout the period of study, supporting, sharing me his knowledge, guiding me and editing my thesis. I also would like to thank the thesis examining committee, including Assoc. Prof. Dr. Jatuporn Wittayakun, Asst. Prof. Dr. Kunwadee Rangsriwatananon and Asst. Prof. Dr. Rapee Utke for their helpful and valuable comments and suggestion during my thesis defense. I would like to thank all lecturers at the School of Chemistry, Suranaree University of Technology for their good attitude and advice.

I would like to thank the staff of the Center for Scientific and Technological Equipment of F2 and F10, Suranaree University of Technology for assisting me with the equipment. Finally, I wish to thank my mother and my sisters for their unconditional love and encouragement during my education.

Wimolmas Siriwanitch

CONTENTS

Page

CHAPTER

CONTENTS (Continued)

CONTENTS (Continued)

Page

LIST OF TABLES

LIST OF FIGURES

Figure **Page**

LIST OF FIGURES (Continued)

Figure **Page**

CHAPTER I

INTRODUCTION

1.1 Significance of the study

Transesterification is a reaction between alkyl alcohol and triglyceride to produce biodiesel. Common sources of triglyceride are vegetable oils, animal fats and waste cooking oils. The reaction is commonly carried out in the presence of an alkaline catalyst such as NaOH and KOH as shown in Figure 1.1. Acid catalysts can also be used but the reaction takes longer time to complete and the acids are corrosive to a reactor. In transesterification with a basic catalyst, free fatty acids (FFA) could react with the catalyst to form soap and water as shown in Figure 1.2. The reaction leads to the formation of emulsion in the biodiesel mixture, which cause a difficulty in the separation of biodiesel from the reaction mixture. The reaction also lowers the amount of the catalyst and consequently, the biodiesel yield is decreased. This problem is significant when the amount of FFA is more than 1 wt% (Gerpen, 2005; Berchmans and Hirata, 2008). Therefore, reduction of FFA in the oils containing high FFA content such as Jatropha curcas seed oil, containing 15 wt% FFA (Berchmans and Hirata, 2008) is necessary.

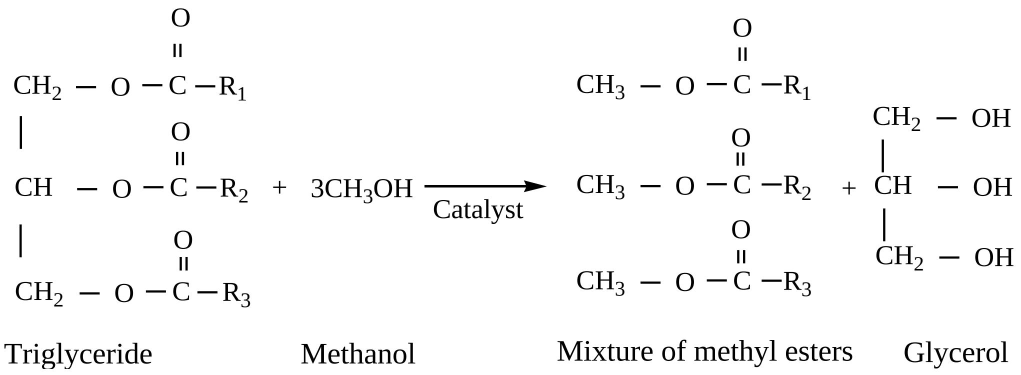

Figure 1.1 Transesterification reaction of triglyceride with methanol. R_1, R_2 and R_3 are alkyl groups with different number of carbon atoms.

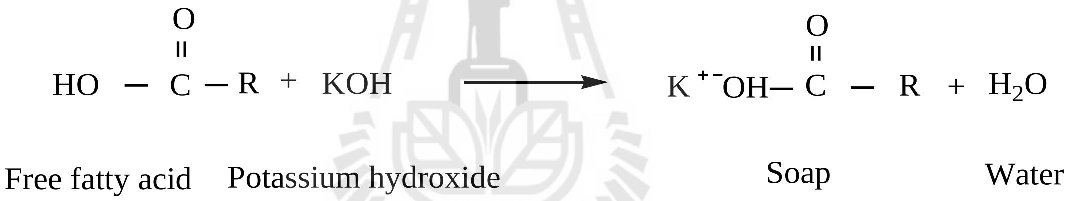

$$HO - \overset{\overset{O}{\|}}{C} - R + KOH \longrightarrow K^{+}\,{}^{-}OH - \overset{\overset{O}{\|}}{C} - R + H_2O$$

Figure 1.2 Reaction of free fatty acid and potassium hydroxide.

1.2 Adsorption

Adsorption is one of the methods used for the removal of FFA in vegetable oils. It has some advantages such as simple operation process, no requirement for sophisticated equipment and relatively inexpensive method. Adsorption process involves the mass transfer of an adsorbate from a fluid phase to the surface of an adsorbent. The adsorbate can physically and chemically interact with the adsorbent. In physical adsorption or physisorption the adsorbent interacts with the adsorbate through electrical forces. The physical adsorption process could be characterized by the heat of adsorption, which is lower than 40 kJ/mol. In contrast, chemical adsorption or chemisorption is a type of adsorption whereby the adsorbate formed a chemical bond with the adsorbent. The heat of adsorption is in a range of 60-400 kJ/mol (Masel, 1996).

1.3 Adsorption isotherms

Adsorption isotherms are used to describe the interaction between the adsorbent in equilibrium with the adsorbate at a constant temperature. There are several theoretical models developed to explain the adsorption process and the commonly used models for adsorption in condensed phase are Langmuir and Freundlich model.

1.3.1 Langmuir isotherm

The Langmuir isotherm describes the adsorption based on the assumption that the surface of the adsorbent is uniform, adsorbed molecules do not interact, all adsorption occurs through the same mechanism and at the maximum adsorption, only a monolayer is formed (molecules of the adsorbate do not deposit on the other). Langmuir adsorption isotherm can be expressed as equation (1)

$$q_e = \frac{q_m K_L C_e}{1 + K_L C_e} \tag{1}$$

where, q_e is the amount of the adsorbate per gram of the adsorbent (mg/g). q_m is the maximum amount of the adsorbate to form a complete monolayer on the surface (mg/g). K_L is the Langmuir adsorption equilibrium constant (L/mg). C_e is the concentration of the adsorbate in a solution at equilibrium (mg/L). Langmuir isotherm can be rearranged to give equation (2)

$$\frac{1}{q_e} = \frac{1}{q_m K_L}\frac{1}{C_e} + \frac{1}{q_m} \tag{2}$$

Accordingly, a plot of $1/q_e$ versus $1/C_e$ produces a straight line with the slope of $1/q_mK_L$ and the intercept of $1/q_m$. The suitability of the adsorption can be evaluated by using Langmuir constant to calculate the factor R_L as described in equation (3)

$$R_L = \frac{1}{(1+K_LC_0)} \tag{3}$$

where, C_0 is the initial concentration of the adsorbate (mg/L). R_L is known as the constant separation factor or equilibrium parameter which indicates the type of adsorption to be either unfavorable (R_L>1), linear (R_L=1), or favorable (0< R_L<1).

1.3.2 Freundlich isotherm

Another commonly used model is Freundlich adsorption isotherm. In contrast to the Langmuir isotherm, the Freundlich isotherm is used to describe a heterogeneous adsorption surface. The isotherm is expressed as equation (4)

$$q_e = K_FC_e^{1/n} \tag{4}$$

q_e and C_e are the same as for equation (1). K_F is the Freundlich constant (function of energy of adsorption and temperature). N is an empirical constant. 1/n indicates the intensity of adsorption or effectiveness of adsorption. When 1/n is less than unity, the adsorption is favorable. Freundlich isotherm can be rearranged to give a linear form in equation (5)

$$\ln q_e = \ln K_F + \frac{1}{n}\ln C_e \tag{5}$$

A plot of $\ln q_e$ versus $\ln C_e$ produces a straight line with the slope of 1/n and the intercept of $\ln K_F$.

1.4 Thermodynamic parameters

Thermodynamic parameters, namely free energy change (ΔG), enthalpy change (ΔH) and entropy change (ΔS) of the adsorption process can be derived from the adsorption study. The ΔG can be calculated from equation (6)

$$\Delta G = -RT \ln K_L \tag{6}$$

where R is the universal gas constant (8.314 J/mol.K). T is the absolute temperature (Kelvin).

The ΔH and ΔS can be determined using the van't Hoff equation (7)

$$\ln K_L = -\frac{\Delta H}{RT} + \frac{\Delta S}{R} \tag{7}$$

A plot of $\ln K_L$ and 1/T yields a straight line, where ΔH and ΔS could be derived. The values of ΔG, ΔH and ΔS indicate the nature of adsorption and are summarized in Table 1.1.

Table 1.1 Relationship of ΔH and ΔS on spontaneity of a process (Zumdahl and Zumdahl, 1989).

ΔH	ΔS	ΔG	Spontaneity of a process
-	+	-	Spontaneous at all temperature
+	-	+	Non- spontaneous
+	+	-	Spontaneous at high temperature
-	-	-	Spontaneous at low temperature

1.5 Adsorbents

Adsorbents play an important role in the adsorption process. Properties of the adsorbents such as surface reactivity, surface area, particle size and porosity would contribute highly on the adsorption capacity. Materials with high porosity and small particle size would provide high probability for physical or chemical interaction with the adsorbate to occur (Masel, 1996).

Sugarcane bagasse (SB) is a residue waste from sugar extraction process. It can be used as a boiler fuel to provide energy for a sugar mill and the by-product of the combustion process is sugarcane bagasse ash (SCBA). SB contains 46% cellulose, 25% hemicelluloses, 20% lignin, 3.5% fat and wax, 2.5% ash, 2% silica and 1.7% other compounds (Homagai, Ghimire and Inoue, 2010). SB has high amount of hydroxyl and phenolic groups that can be modified (Yu, Wang, Chi, Zhang, Xu and Guo, 2013). SCBA composes of about 80% SiO_2 and other metal oxides such as Al_2O_3, Fe_2O_3 and CaO (Zandeson, Gravitis, Kokorevics, Zhurinsh, Bikovens, Tardenaka and Spince, 1999).

There are many methods such as physical, physical-chemical and chemical treatment to modify the property of adsorbents from lignocellulosic materials. A common method to extract cellulose from lignocellulosic materials such as SB is acid leaching treatment. H_2SO_4 can be used to break down cellulose material into a small fragment that results in an increase proportion of active surfaces (Martín-Lara, Rico, Vicente, Garcia and Hoces, 2010) and eliminates soluble components, such as tannins, resins, reducing sugars and coloring agents. Another method to remove some organic content is a burning method (Umeda, Kondoh and Michiura, 2007). An alkali extraction under low temperature was also used to dissolve silica from lignocellulosic materials

(Affandi, Setyawan, winardi, Purwanto and Balgis, 2009).

In this research adsorbents were obtained from the modification of SB and SCBA. SB was treated with acid, heat or both and SCBA was hydrothermally treated in basic solutions. SB, SCBA and the treated materials were used in the adsorption of oleic and capric acid. Some of the derived materials were characterized using various techniques to provide information about the properties of the materials that were used to relate with their adsorption efficiency. Influence parameters on the adsorption capacity such as acid concentration, amount of adsorbent, and temperature were investigated. Experimental data were correlated with isotherm models to explain the adsorption nature of the studied systems.

1.6 References

Affandi, S., Setyawan, H., Winardi, S., Purwanto, A. and Balgis, R. (2009). A facile method for production of high-purity silica xerogels from bagasse ash. **Advanced Powder Technology**. 20: 468-472.

Berchmans, H. J. and Hirata, S. (2008). Biodiesel production from crude Jatrophacurcas L. seed oil with a high content of free fatty acids. **Bioresource Technology**. 99: 1716-1721.

Gerpen, J. V. (2005). Biodiesel processing and production. **Fuel Processing Technology**. 86: 1097-1107.

Homagai, P. L., Ghimire, K. N. and Inoue, K. (2010). Adsorption behavior of heavy metals onto chemically modified sugarcane bagasse. **Bioresource Technology**. 101: 2067-2069.

Martín-Lara, M. A., Rico, I .L. R., Vicente, I. C. A., García, G. B. and Hoces, M. C. (2010). Modification of the sorptive characteristics of sugarcane bagasse for removing lead from aqueous solutions. **Desalination**. 256: 58-63.

Masel, R. I. (1996). **Principles of adsorption and reaction on solid surfaces**. John Wiley & Sons: Canada, pp. 111-112.

Umeda, J., Kondoh, K. and Michiura, Y. (2007). Process parameters optimization in preparing high-purity amorphous silica originated from rice husks. **Materials Transactions**. 48: 3095-3100.

Yu, J. X., Wang, L. Y., Chi, R. A., Zhang, Y. F., Xu, Z. G. and Guo, J. (2013) Competitive adsorption of Pb^{2+} and Cd^{2+} on magnetic modified sugarcane bagasse prepared by two simple steps. **Applied Surface Science**. 268: 163-170.

Zandersons, J., Gravitis, J., Kokorevics, A., Zhurinsh, A., Bikovens, O., Tardenaka, A. and Spince, B. (1999). Studies of the Brazilian sugarcane bagasse carbonisation process and products properties. **Biomass and Bioenergy**. 17: 209-219.

Zumdahl, S. S. and Zumdahl, S. A. (1989). **Chemistry**. 2nd ed., D.C. Heath: Lexington, MA, pp. 737-771.

CHAPTR II

LITERATURE REVIEWS

2.1 Introduction

Free fatty acids (FFA) in vegetable oils can be derived from triglycerides consisting of different fatty acid (FA) moieties which vary according to their origins. Parameters that could influence the FA composition of triglycerides are for example, vegetable matrix (fruit or seed), climatic condition and harvest time. (Guarrasi, Mangione, Sanfratello, Martorana and Bulone, 2010). FA compositions of some vegetable oils are summarized in Table 2.1. C18:1 fatty acid is among the most abundant compositions in the vegetable oils; therefore in this research, oleic acid was selected as a representative of FFA for the adsorption study.

There are many methods to remove various FFA from oils such as esterification, distillation, membrane separation and adsorption. In esterification, FFA reacts with alcohol in the presence of an acid catalyst to produce esters. Berchmans and Hirata (2008) removed FFA in crude Jatropha curcas seed oil containing 15 wt% FFA by esterification at 50 ^oC for 1 h using 0.60 w/w methanol-to-oil ratio in the presence of 1 wt% H_2SO_4 as a catalyst. This method reduced FFA to less than 1 wt%.

Table 2.1 Fatty acid composition (wt%) of some common edible oils (Ramos, Fernandez, Casas, Rodriguez and Perez, 2009).

Fatty acid (Cn:x)[a]	Palm	Olive	Peanut	Soybean	Sunflower	Corn
Lauric (C12:0)	0.1	0.0	0.0	0.0	0.0	0.0
Myristic (C14:0)	0.7	0.0	0.1	0.0	0.0	0.0
Palmitic (C16:0)	36.7	11.6	8.0	11.3	6.2	6.5
Palmitoleic (C16:1)	0.1	1.0	0.0	0.1	0.1	0.6
Stearic (C18:0)	6.6	3.1	1.8	3.6	3.7	1.4
Oleic (C18:1)	46.1	75.0	53.0	24.9	25.2	65.6
Linoleic (C18:2)	8.6	7.8	28.4	53.0	63.1	25.2
Linolenic (C18:3)	0.3	0.6	0.3	6.1	0.2	0.1
Arachidic (C20:0)	0.4	0.3	0.9	0.3	0.3	0.1
Gadoleic (C20:1)	0.2	0.0	2.4	0.3	0.2	0.1
Behenic (C22:0)	0.1	0.1	3.0	0.0	0.7	0.0
Erucic(C22:1)	0.0	0.0	0.0	0.3	0.1	0.1
Lignoceric (C24:0)	0.1	0.5	1.8	0.1	0.2	0.1
Nervonic (C24:1)	0.0	0.0	0.0	0.0	0.0	0.0

[a] Cn represents number of carbon atoms and x is a number of double bonds in the acid molecule.

Sathya Selva Bala, Thiruvengadaravi, Senthil Kumar, Premkumar, Vinothkumar, Subashsankar, Hari Kumar and Sivanesan (2012) removed FFA in Pongamia Pinnata (Karanja) oil having 6.3 wt% FFA by esterification using acidic ion-exchange resins (Amberlite IR 120 H and Amberjet 1200 H) as the catalysts. Parameters for the reaction were methanol-to-oil molar ratio 6:1, reaction temperature 60 °C, reaction time 25 min and the catalyst amount of 0.8 wt% for Amberlite IR120 H and 1 wt% for Amberjet 1200 H. The amount of FFA was reduced to lower than 1 wt%.

In distillation method, FFA is separated from the oils by the differences between molecular weights and vapor pressures. Martins, Ito, Batistella and Maciel (2006) and Posada, Shi, Kakuda and Xue (2007) used molecular distillation process to separate FFA from soybean oil deodorizer distillate, containing 58 wt% FFA and palm fatty acid distillate, respectively. Distillation could remove FFA more than 95 wt%.

Membrane filtration is a size-exclusion based pressure-driven process that separates components according to molecular weights, particle sizes and shapes. Zwijnenberg, Krosse, Ebert, Peinemann and Cuperus (1999) used nanofiltration hydrophilic membranes modified the top layer with poly (amide-b-ether) copolymer and cellulose to separate FFA in palm, rapeseed and sunflower oil. The filtration method could remove about 45-60 wt% FFA from the oils. Moura, Goncalves, Petrus and Viotto (2005) used ultrafiltration membrane from polyethersulphone to separate FFA in crude soybean oil. This membrane could remove about 21 wt% FFA from the oil. Ribeiro, Bei, Goncalves, Petrus and Viotto (2008) investigated ceramic membrane modified the top layer with an active alumina layer to separate FFA in soybean oil. This method could remove FFA about 12 wt%.

Adsorption is another method for the removal of FFA. It has some advantages including simple operation process and low cost. Many adsorbents have been investigated for the removal of FFA. Lin, Akoh and Reynolds (1999) used commercial adsorbents such as Britsorb (silicon dioxide mixed with aluminum hydroxide), Hubersorb 600 (calcium silicate), Frypower (porous rhyolite and citric acid), Magnesol (magnesium silicate) and combination of these adsorbents for FFA removal in frying oils. Kheang, Subari and Kadir (2011) studied the adsorption of FFA in palm olein derived used frying oil by activated carbon, activated bleaching earth, silica gel and aluminium oxide. The most effective adsorbent was silica gel followed by activated carbon, activated bleaching earth and aluminium oxide. Adsorption by silica gel followed Freundlich adsorption isotherm and the adsorption occurred via the interaction between the polar carbonyl groups of the acids and hydrophilic silanol (-Si–OH) and siloxane (-Si–O–Si-) groups of the adsorbent. Sathivel and Prinyawiwatkul (2004) investigated chitosan, activated carbon and activated earth as adsorbents to remove FFA from crude catfish visceral oil. Chitosan had the highest adsorption capacity. Maddikeri, Pandit and Gogate (2012) investigated adsorption of stearic and oleic acid in refined sunflower oil on weak anion-exchange resins (Indion 850 and 860) and strong anion-exchange resin (Indion 810). They observed that adsorption increased with the concentration of the fatty acids at a constant temperature and decreased with increase temperature at constant concentration and the adsorption was spontaneous and exothermic. The adsorption followed Freundlich isotherm.

Adsorbents obtained from rice husk silica have been studied for FFA adsorption. Farook and Ravendran (2000) evaluated the adsorption capacity of acid treated rice husk ash. The treatment of the rice husk ash with nitric acid increased the surface area of the ash and consequently, enhanced the adsorption capacity. Kalapathy and Proctor (2000) used sodium silicate films synthesized from rice husk silica to reduce FFA in frying oil. Decrease of FFA in the oil was achieved with increasing treatment time and the amount of the adsorbent used. Meanwhile, the soap content in the oil also increased. Özgül-Yücel and Türkay (2003) compared FFA adsorption capacities of rice husk ash and silica gel in fatty acid methyl ester mixture. They found that rice husk ash calcined at 500 ^{o}C had lower adsorption capacity than the silica gel. Yoon, Kim and Gil (2011) calcined rice husk ash in the temperature range 300-900 ^{o}C and used the obtained ashes as adsorbents for FFA. Heat treatment caused the change in the adsorbent structures and affected the adsorption capacity. The researchers also treated rice husk ash that calcined at 500 ^{o}C with sulfuric acid and found that the adsorption capacity for FFA of the derived adsorbent was not significantly different from that of the nontreated rice husk ash calcined at the same temperature.

Recently, Ali and Anany (2012) reported the used SCBA to recover the used frying sunflower oil compared the results with the study using Magnesol XL (synthetic magnesium silicate) as the adsorbent. SCBA was prepared by carbonization of SB in air at 650 ^{o}C for 12 h. The carbonized SB composed of about 77 wt% SiO_2 and other metal oxides such as CuO, Fe_2O_3, CaO, K_2O, MgO and Na_2O. These adsorbents could reduce FFA in the oil but increased the soap content due to the reaction of FFA with sodium silicate.

In this work adsorbents derived from SB and SCBA was investigated for the adsorption of oleic acid. It was expected that the organic functional groups and silicon compounds in the SB and SCBA would be useful for the adsorption of free fatty acids.

2.2 References

Ali, R. F. M. and Anany, A. M. E. (2012). Recovery of used frying sunflower oil with sugarcane industry waste and hot water. **Journal of Food Science and Technology**. 51(11): 3002-3013.

Berchmans, H. J. and Hirata, S. (2008). Biodiesel production from crude Jatropha curcas L. seed oil with a high content of free fatty acids. **Bioresource Technology**. 99: 1716-1721.

Farook, A. and Ravendran, S. (2000). Saturated fatty acid adsorption by acidified rice hull ash. **Journal of the American Oil Chemists' Society**. 77: 437-440.

Guarrasi, V., Mangione, M. R., Sanfratello, V., Martorana, V. and Bulone, D. (2010). Quantification of underivatized fatty acids from vegetable oils by HPLC with UV detection. **Journal of Chromatographic Science**. 48: 663-668.

Kalapathy, U. and Proctor, A. (2000). A new method for free fatty acid reduction in frying oil using silicate films produced from rice hull ash. **Journal of the American Oil Chemists' Society**. 77: 593-598.

Kheang, L. S., Subari, F. and Kadir, S. A. S. (2011). Pre-treatment of palm olein-derived used frying oil as feedstock for non-food applications. **Journal of Oil Palm Research**. 23: 1185-1192.

Lin, S., Akoh, C. C. and Reynolds, A. E. (1999).Determination of optimal conditions for selected adsorbent combinations to recover used frying oils. **Journal of the American Oil Chemists' Society**. 76: 739-744.

Maddikeri, G. L., Pandit, A. B. and Gogate, P. R. (2012). Adsorptive removal of saturated and unsaturated fatty acids using ion-exchange resins. **Industrial Engineering Chemistry Research**. 51: 6869-6876.

Martins, P. F., Ito, V. M., Batistella, C. B. and Maciel, M. R. W. (2006). Free fatty acid separation from vegetable oil deodorizer distillate using molecular distillation process. **Separation and Purification Technology**. 48: 78-84.

Moura, J. M. L. N., Goncalves, L. A. G., Petrus, J. C. C. P. and Viotto, L. A. (2005). Degumming of vegetable oil by microporous membrane. **Journal of Food Engineering**. 70: 473-478.

Özgül-Yücel, S. and Türkay, S. (2003). Purification of FAME by rice hull ash adsorption. **Journal of the American Oil Chemists' Society**. 80: 373-376.

Posada, L. R., Shi, J., Kakuda, Y. and Xue, S. J. (2007). Extraction of tocotrienols from palm fatty acid distillates using molecular distillation. **Separation and Purification Technology**. 57: 220-229.

Ramos, M. J., Fernández, C. M., Casas, A., Rodríguez, L. and Pérez, A. (2009). Influence of fatty acid composition of raw materials on biodiesel properties. **Bioresource Technology**. 100: 261-268.

Ribeiro, A. P. B., Bei, N., Goncalves, L. A. G., Petrus, J. C. C. P. and Viotto, L. A. (2008). The optimisation of soybean oil degumming on a pilot plant scale using a ceramic membrane. **Journal of Food Engineering**. 87: 514-521.

Sathivel, S. and Prinyawiwatkul, W. (2004). Adsorption of FFA in crude catfish oil onto chitosan, activated carbon, and activated earth: a kinetics study. **Journal of the American Oil Chemists' Society**. 81: 493-496.

Sathya Selva Bala, V. S. S., Thiruvengadaravi, K. V., Kumar, P. S., Premkumar, M. P., Kumar, V. V., Sankar, S. S., Kumar, M. H. and Sivanesan, S. (2012). Removal of free fatty acids in Pongamia Pinnata (Karanja) oil using divinylbenzene-styrene copolymer resins for biodiesel production. **Biomass and Bioenergy**. 37: 335-341.

Yoon, S. H., Kim, M. and Gil, B. (2011). Deacidification effects of rice hull-based adsorbents as affected by thermal and acid treatment. **LWT-Food Science and Technology**. 44: 1572-1576.

Zwijnenberg, H. J., Krosse, A. M., Ebert. K., Peinemann, K. V. and Cuperus, F. P. (1999). Acetone-stable nanofiltration membranes in deacidifying vegetable oil. **Journal of the American Oil Chemists' Society**. 76: 83-87.

CHAPTER III

EXPERIMENTAL

3.1 Chemicals and equipment

3.1.1 Chemicals

Chemicals used in this research were purchased from various suppliers as shown in Table 3.1. All chemicals were used as received with no further purification.

Table 3.1 Chemicals used in the research.

Chemicals	Suppliers	Purity (%)
acetonitrile	Carlo Erba	99.9, HPLC grade
capric acid	Sigma-Aldrich	98
ethanol	Carlo Erba	99.9
glacial acetic acid	Baker Analyzed	99.9
isooctane	Carlo Erba	99.9, HPLC grade
isopropyl alcohol	Carlo Erba	99.7
methanol	Carlo Erba	99.9
oleic acid	Sigma-Aldrich	90
phenolphthalein	QRëc	-
potassium hydrogen phthalate	Sigma-Aldrich	100.05
potassium hydroxide (KOH)	QRëc	85.0
sodium hydroxide (NaOH)	QRëc	96

Table 3.1 Chemicals used in the research. (Continued)

Chemicals	Suppliers	Purity (%)
sulfuric acid (H_2SO_4)	QRëc	96
toluene	Carlo Erba	99.5

3.1.2 Equipment

List of equipment used in the research is shown in Table 3.2.

Table 3.2 Equipmentused in this research.

Equipment	Suppliers
analytical balance	Presica 250, Presica
centrifuge machine	Z206A, HERMLE
desiccator	Patron Dry-Cabinet
Fourier transform infrared spectrometer	TENSOR 27, Bruker
glass syringe	Comet
heating mantle	Lab Heat
high pressure liquid chromatograph	HPLC 1260, Agilent
hot air oven	Memmert
laboratory blender	Waring Comercial
muffle furnace	CWF1200, Carbolite
multichannel stirrer	Diligent
nitrogen adsorption-desorption analyzer	BEL Japan
scanning electron microscope	JSM 6010 LV, JEOL
standard sieve	Analysensieb Restch
temperature-controlled water bath	Heto Equipment

Table 3.2 Equipment used in this research. (Continued)

Equipment	Suppliers
vacuum filtration apparatus	Millipore
x-ray fluorescence spectrometer	PANalytical, AXIOS
x-ray powder diffractometer	Bruker, D2 PHASER

3.2 Preparation of adsorbents

Sugarcane bagasse (SB) was obtained from local sugarcane juice shops in Nakhon Ratchasima province. SB was cut, blended and washed thoroughly with water. After that, the SB was dried in an oven at 50 °C and sieved to particle sizes in the range of 1.0-2.36 mm.

To produce an acid-treated SB, a procedure modified from the literature (Lacerda, Zambon and Frollini, 2013) was followed. SB was refluxed with 6 M H_2SO_4 in a round-bottom glass flask at 100 °C for 6 h. After that, the solid was separated by filtration and washed with water until the washing liquid had the pH ~7. The SB treated with H_2SO_4 was then dried in an oven at 50 °C, sieved to the particle sizes of 75-90 µm and kept in an airtight desiccator. The acid treated SB was called SB-H_2SO_4. For heat treatment, SB and SB-H_2SO_4 were calcined at 400 °C or 500 °C in a muffle furnace with a heating rate of 2 °C/min for 3 h and the obtained solids calcined at 400 °C were called SB-400 and SB-H_2SO_4-400; and those calcined at 500 °C were called SB-500 and SB-H_2SO_4-500. After calcination, the obtained solids were sieved to the particle sizes of 75-90 µm. The calcined products were kept in an airtight desiccator.

Sugarcane bagasse ash (SBCA) was obtained from Surin Sugar Company, Surin province. SCBA was washed with water to remove adhering soil and dust and dried in an oven at 50 °C.

For base-treated SCBA, a modified procedure from the literature (Shah, Mistry and Shah, 2013) was used. SCBA was soaked with 6 M NaOH in a plastic bottle at room temperature with stirring provided. The ratio of the alkali solution volume to the mass of solid was 10:1 (mL:g). The soaking time was varied in the range of 1 to 6 h. After the given time, solid particles were separated by filtration, washed with water until the pH of the washed solution was ~7 and dried in the oven at 50 °C. The obtained adsorbents were sieved to the particle sizes in the range of 75-90 µm and stored in an airtight desiccator. SCBA treated with NaOH at 1, 2, 3 and 6 h were denoted as SCBA-NaOH-1h, SCBA-NaOH-2h, SCBA-NaOH-3h and SCBA-NaOH-6h, respectively.

In hydrothermal treated SCBA, a modified procedure from the literature (Shah, Tailor and Shah, 2012) was used. SCBA was soaked with 6 M NaOH in a Tefflon container at room temperature for 1 h with stirring provided. After that the container was placed in an autoclave and put into a hot air oven at 100 °C for 72 h. After the given time, solid particles were separated by filtration, washed with water until the neutral pH of the filtrate was observed and dried in the oven at 50 °C. The obtained adsorbents were sieved to the particle sizes in the range of 75-90 µm and stored in an airtight desiccator. Hydrothermally treated SCBA was denoted as SCBA-hydrothermal.

3.3 Characterization of adsorbents

3.3.1 Powder X-ray diffraction (XRD)

Powder XRD patterns were obtained with a diffractometer using a Ni-filtered Cu Kα (λ= 1.54056 Å) radiation source with the current of 10 mA and the voltage of 30 kV. The XRD patterns were recorded at room temperature between 10 °

to 70 ^{o} (2θ) and a scan speed of 0.2 degree/s.

3.3.2 X-ray fluorescence spectroscopy (XRF)

Elemental compositions of the adsorbents were determined by using a wavelength dispersive X-ray fluorescence spectrometer. An X-ray source was Rh X-ray tube targeted with a collimator size 150 µm. A sample holder with an optical path diameter of 37 mm was used for the measurement. The X-ray generator was operated at the voltage of 50 kV and the current of 60 mA.

3.3.3 Scanning electron microscopy (SEM)

Morphologies of the adsorbents were obtained using a scanning electron microscope. Adsorbents specimens were gold coated in an ion sputtering device for 8 min at 10 mA current output. The scanning electron microscope was operated at 15 kV and a working distance of 10 mm. Areas of interest were focused and micrographs were taken.

3.3.4 N_2 adsorption-desorption analysis

Textural properties of the adsorbents were determined by N_2 adsorption-desorption analysis at temperature of liquid nitrogen -196 ^{o}C for relative pressure from 0.001 to 0.99 on an N_2 gas analyzer. Before the measurement, the 150-250 mg of sample was degassed at 150 ^{o}C for 12 h. The specific surface area (S_{BET}) was calculated by a Brunauer-Emmet-Teller (BET) method in the relative pressure range of 0.001-0.990. The total pore volume was calculated using a Barrette-Joyner-Halenda (BJH) method.

3.3.5 Fourier transform infrared spectroscopy (FT-IR)

Functional groups on the adsorbents were characterized by an FTIR spectrometer with a KBr technique. KBr was dried at 110 ^{o}C for 12 h to remove humidity. About 3 mg of an adsorbent was mixed with 30 mg KBr and the mixture was ground in a mortar. The powder was transferred into a sample barrel and pressed with 13 tons of force for 1 min to form a pellet and put on a V-mount sample holder. The range of measurement was 4000-400 cm^{-1}. The spectra were obtained by using an average of 10 scans with 4 cm^{-1} resolution.

3.4 Preparation of solutions

Potassium hydroxide was used for the titration of oleic and capric acid. A stock solution of 0.1 M KOH was prepared by dissolving 1.65 g KOH in CO_2-freed deionized water and adjusting the volume to 250 mL in a volumetric flask. A solution of 0.01 M KOH was prepared by the dilution of the 0.1 M KOH solution. The KOH solutions were standardized with potassium hydrogen phthalate using 1% phenolphthalein solution as the indicator.

A mixture of toluene and isopropanol with 1:1 volume ratio was used as a solvent for the titration of oleic and capric acid in isooctane and in vegetable oil. Before using in the titration, the solution was neutralized with a standardized 0.1 M KOH using phenolphthalein as the indicator.

Phenolphthalein was used as an indicator for the titration of KOH and oleic or capric acid. To prepare 1 %w/v phenolphthalein, 1.0 g of phenolphthalein was dissolved in 50 mL of ethanol. The solution was transferred into a 100 mL volumetric flask and the volume of the solution was adjusted with CO_2-free deionized water.

Solutions of oleic and capric acid were prepared using isooctane as a solvent. The concentration of acid was in the range of 0.05-2.0 %w/v.

3.5 Adsorption studies

All the adsorption studies were carried out by batch technique. A 25 mL of an acid solution in isooctane was mixed with 0.20 g of an adsorbent in 125 mL erlenmeyer flask with a screw cap. The sample was stirred for 30 min in a temperature-controlled water bath at 25, 35 and 45 ^{o}C and then left unstirred for 30 min. The adsorbent was separated by filtration with 0.45 µm nylon membrane before the determination of acids.

To study adsorption capacities of hydrothermal treated SCBA, a 25 mL of 1.0 %w/v oleic or capric acid solution in soybean oil was mixed with 0.20 g of an adsorbent in 125 mL erlenmeyer flask with a screw cap. The sample was stirred for 30 min in a temperature-controlled water bath at 25 ^{o}C and then left unstirred for 30 min. The adsorbent was separated by centrifugation before the determination of oleic or capric acid.

3.6 Determination of oleic and capric acid

3.6.1 High performance liquid chromatography (HPLC)

The concentration of oleic acid was determined by using HPLC with a modified procedure from the literature (Guarrasi, Mangione, Sanfratello, Martorana and Bulone, 2010). A column used in the analysis was Hypersil ODS C-18. A mobile phase was acetonitrile mixed with 0.4% acetic acid with the volume ratio of 90:10. A detector was a UV spectrometer recording absorbance at 195 nm.

3.6.2 Titration

The amount of oleic acid and capric acid was determined by titration according to the American Oil Chemists' Society method (AOCS Ca 5a 40), which 1 mL of the oleic or capric acid solution was mixed with 25 mL solution of toluene mixed with isopropyl alcohol (1:1 v/v). The mixture was titrated with the standardized 0.01 M KOH using phenolphthalein as the indicator. The adsorption capacity was calculated according to equation (8),

$$q = \frac{V(C_o - C_e)}{M} \tag{8}$$

where q is the adsorption capacity (mg/g), V is the volume of oleic or capric acid solution (L), C_o and C_e are the initial and equilibrium concentration of oleic or capric acid (mg/L) and M is the mass of the adsorbent (g).

3.7 References

Guarrasi, V., Mangione, M. R., Sanfratello, V., Martorana, V. and Bulone, D. (2010) Quantification of underivatized fatty acids from vegetable oils by HPLC with UV detection. **Journal of Chromatographic Science**. 48(8): 663-668.

Lacerda, T. M., Zambon, M. D. and Frollini, E. (2013) Effect of acid concentration and pulp properties on hydrolysis reactions of mercerized sisal. **Carbohydrate Polymers**. 93: 347-356.

Shah, B., Mistry, C. and Shah, A. (2013) Seizure modeling of Pb(II) and Cd(II) from aqueous solution by chemically modified sugarcane bagasse fly ash: isotherms, kinetics, and column study. **Environmental Science and Pollution Research**. 20: 2193-2209.

Shah, B., Tailor, S. and Shah, A. (2012) Zeolitic bagasse fly ash as a low-cost sorbent for the sequestration of p-nitrophenol: equilibrium, kinetics, and column studies. **Environmental Science and Pollution Research**. 19: 1171-1186.

CHAPTER IV

RESULTS AND DISCUSSION

4.1 Characterization of adsorbents from SB

XRD patterns ofSBand SB-H_2SO_4 are shown in Figure 4.1. Diffraction peaks at 2θ ~16° and ~22° are characteristic feature of cellulose (Pereira,Voorwald, Cioffi, Mulinari, Luz and Silva, 2011). When SB was treated with H_2SO_4, the crystalline structure of cellulose almost disappeared indicating that thestructure of cellulose was destroyed from the hydrolysis of the glycosidic bond. (Chen, Tu and Sheen, 2011). The break down of cellulose caused charring of organics (cellulose, hemi-celluloses and lignin) resulting black particles (Umeda, Kondon and Michiura, 2007) and decreased the amount of some metal ions.

Calcination of SB at 400 (SB-400) and 500 °C (SB-500) resulted in grayish white and grey particles, respectively. The calcination process decreased the amount of volatile materials and organic compounds. The XRD patterns of SB-400 and SB-500 are shown in Figure 4.2. SB-400 and SB-500 have mixed phases of quartz (Teixeira, Souza, Santos and Peña, 2008) and amorphous silica (Le Blond, Horwell, William and Oppenheimer, 2010).

For the adsorbents obtained from SBs treated with H_2SO_4 and calcined at 400 (SB-H_2SO_4-400) and 500 °C (SB-H_2SO_4-500), the color of the obtained solid was greyish black. The XRD patterns of SB-H_2SO_4-400 and SB-H_2SO_4-500 shown in Figure 4.3 suggested the presence of calcite (Freire and Holanda, 2006) and anhydrite,

$CaSO_4$, (Gastaldi, Boccaleri, Canonico and Bianchi, 2007). Calcite is the most stable form of $CaCO_3$, which could be decomposed at 500 °C. The presence of anhydrite, could be from the treatment of SB with H_2SO_4.

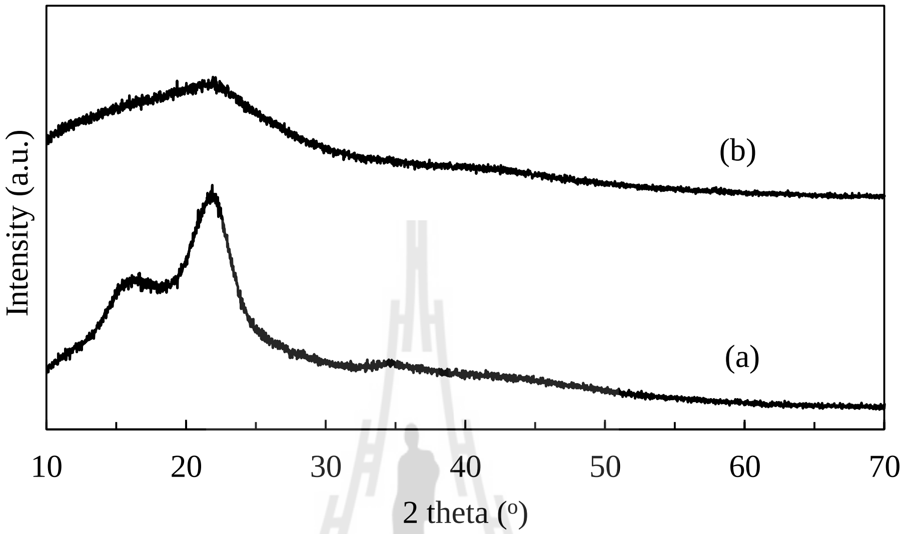

Figure 4.1 The XRD patterns of (a) SB and (b) SB-H_2SO_4.

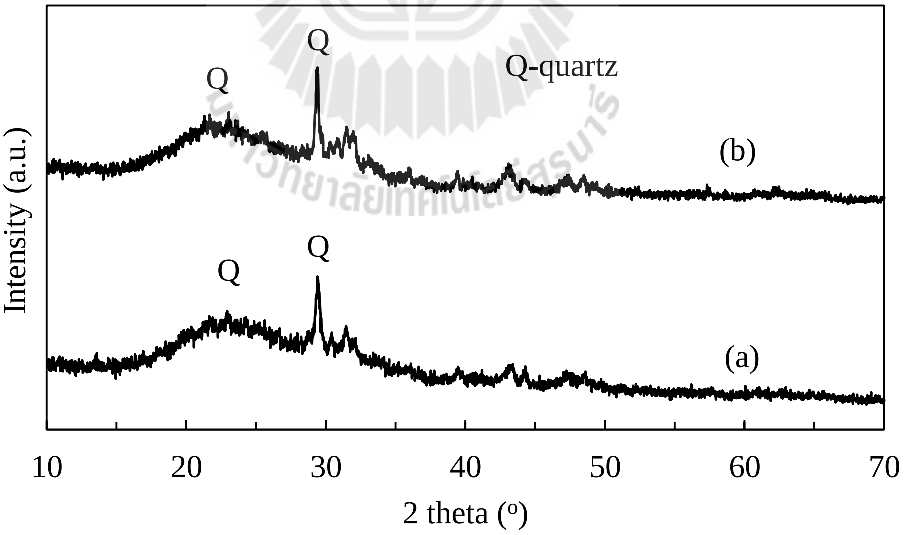

Figure 4.2 The XRD patterns of (a) SB-400 and (b) SB-500.

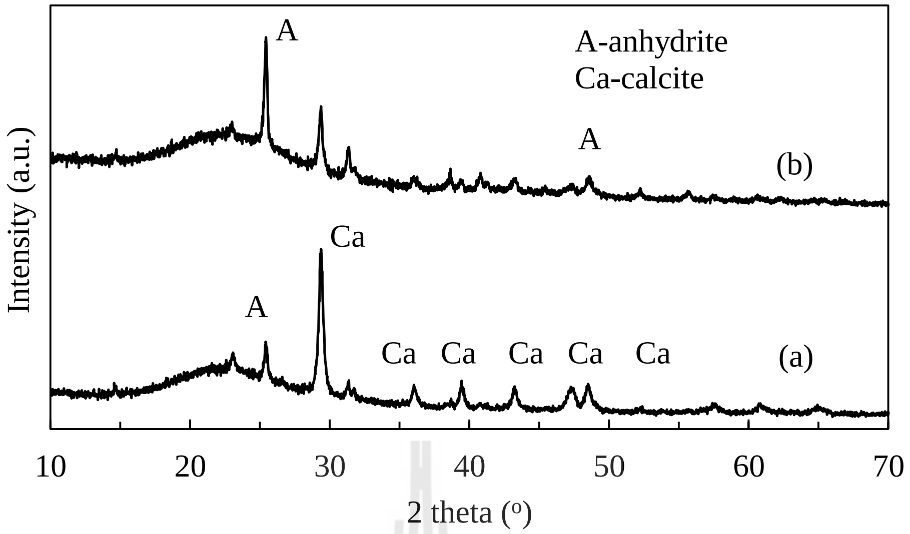

Figure 4.3 The XRD patterns of (a) SB-H_2SO_4-400 and (b) SB-H_2SO_4-500.

Elemental compositions (noncarbonaceous content) of the adsorbents from SBs were determined by XRF and the results are shown in Table 4.1. The major components were Si and Ca. Acid and heat treatment of SB seem to have less effect on the elemental composition of the materials. Some metal contents tend to be reduced after treatment with the acid.

A technique of scanning electron microscopy (SEM) was used to obtain the images of SB and SB treated with H_2SO_4. The results are shown in Figure 4.4. SB has relatively large particles associated with pith structures and vascular bundles. After treatment with acid and calcination or calcination only, the obtained particles have smaller size with wide range of structures. The results suggest that the treatment of SB should provide the adsorbents with higher surface area for the adsorption.

Table 4.1 Chemical compositions of adsorbents from SB determined by XRF.

Component	SB-H_2SO_4-400	SB-H_2SO_4-500	SB-400	SB-500
Na_2O	0.19	0.21	0.44	0.39
MgO	1.18	0.89	1.77	1.42
Al_2O_3	0.11	0.09	0.55	0.13
SiO_2	45.25	37.76	29.82	36.83
P_2O_5	0.93	1.20	6.15	5.19
SO_3	9.65	17.38	6.03	8.12
Cl	0.45	0.39	0.55	0.32
K_2O	1.20	1.79	17.23	16.84
CaO	40.55	38.68	34.77	29.62
Cr_2O_3	0.04	0.31	0.06	0.05
MnO	0.04	-	1.22	0.16
Fe_2O_3	0.38	0.90	1.19	0.70
NiO	-	-	0.04	0.04
CuO	0.03	-	0.20	0.17

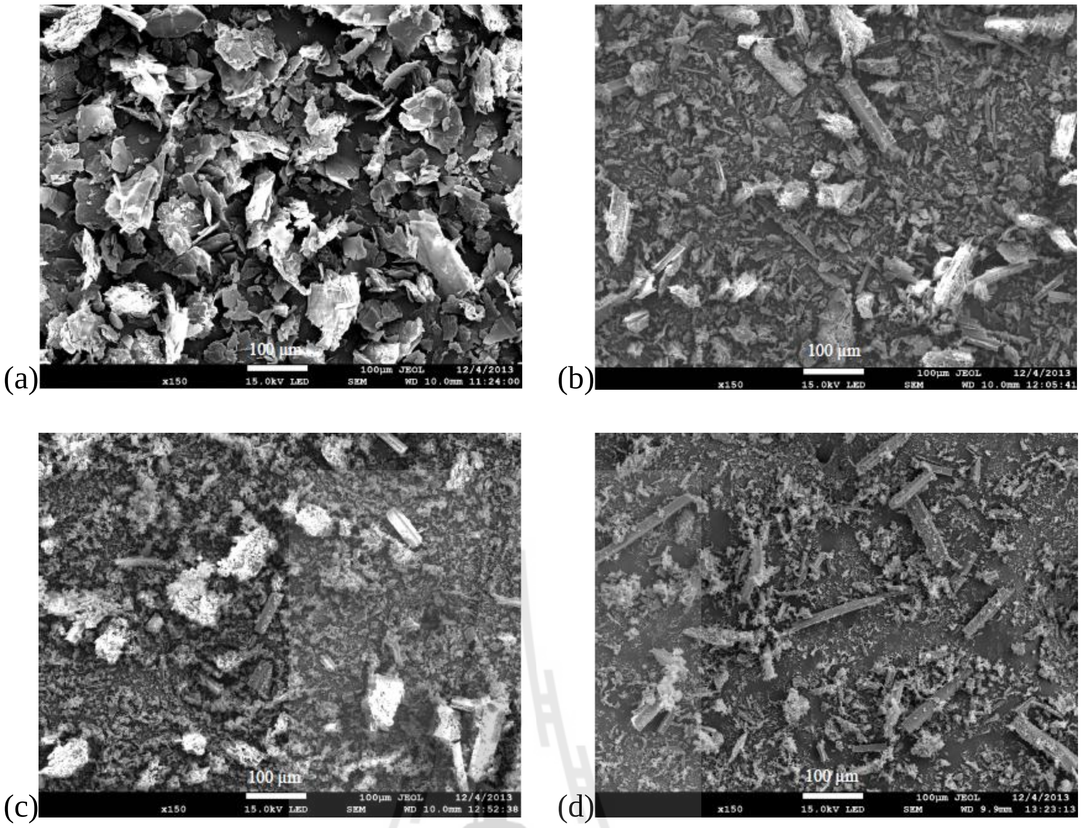

Figure 4.4 SEM images of (a) SB, (b) SB-H_2SO_4, (c) SB-H_2SO_4-500 and (d) SB-500 with a magnification of 150x. The scale bars on the images represent the length of 100 µm. SB-H_2SO_4-500 and SB-500 images of higher magnification are shown in Appendix A.

4.2 Characterization of adsorbents from SCBA

XRD patterns of SCBA and SCBA treated with 6 M NaOH for 1 to 6 h are shown in Figure 4.5. All adsorbents have similar XRD patterns. The major phases were quartz and amorphous silica (Teixeira, Souza, Santos and Peña, 2008). The intensity of quartz increased when treated SCBA with the NaOH solution as a result of the dissolution of amorphous silica from SCBA. Treatment of SCBA with the NaOH solution longer than 1 h seem not to affect for the structure of SCBA. Hydrothermal treatment of SCBA in

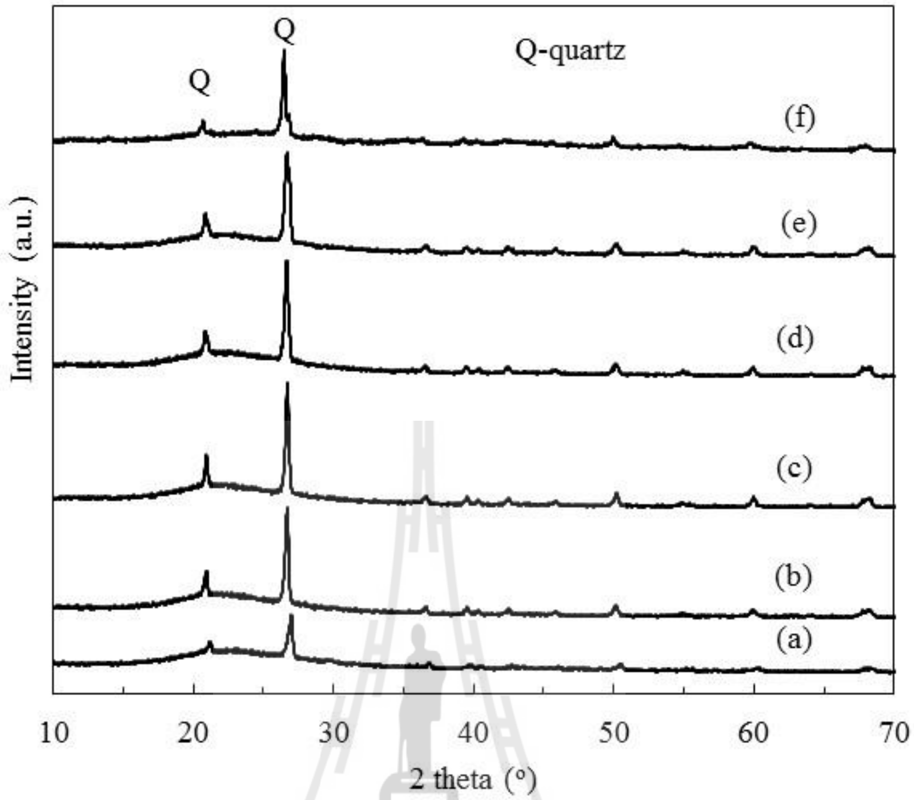

Figure 4.5 The XRD patterns of (a) SCBA, (b) SCBA-NaOH-1h, (c) SCBA-NaOH-2h, (d) SCBA-NaOH-3h, (e) SCBA-NaOH-6h and (f) SCBA-hydrothermal.

the NaOH solution also shows similar XRD pattern as those treated with the NaOH solution at various times.

Elemental composition of SCBA and treated SCBA determined by XRF are shown in Table 4.2. Si was the major component found in the adsorbents. Treating SCBA with NaOH solution for 1 and 6 h tends not to change the composition of the particles. However, when SCBA was treated with NaOH solution under hydrothermal condition at 100 ^{o}C for 72 h the Si content was reduced. This could be resulted from the dissolution of amorphous silica (Shan, Mistry and Shan, 2013).

Table 4.2 Chemical compositions of adsorbents from SCBA determined by XRF.

Component	SCBA	SCBA-NaOH-1h	SCBA-NaOH-6h	SCBA-hydrothermal
Na_2O	-	-	-	0.08
MgO	0.79	0.47	0.53	2.66
Al_2O_3	1.32	1.29	1.39	3.56
SiO_2	63.61	79.97	76.29	48.80
P_2O_5	5.31	2.84	3.72	4.45
SO_3	0.86	0.697	0.90	1.88
Cl	0.58	0.30	0.50	0.71
K_2O	6.06	3.94	4.14	0.60
CaO	14.27	4.10	4.90	10.63
TiO_2	-	0.91	1.06	3.42
Cr_2O_3	0.81	-	-	0.09
MnO	1.43	0.63	0.70	3.96
Fe_2O_3	4.80	4.77	5.76	18.77
NiO	0.04	0.02	0.03	0.11
CuO	0.07	0.07	0.08	0.22
ZnO	0.05	-	-	0.07

SEM images of all the adsorbents from SCBA with 150x and 1000x magnification are shown in Figure 4.6. Wide range of structures are observed. Fibrous particles are obviously present due to the origin of the ash contained mainly fibers (Paya´, Monzo´, Borrachero, Dı´az-Pinzo´n and Ordo´n˜ez, 2002). The treated SCBAs tend to have smaller particle sizes than the untreated SCBA.

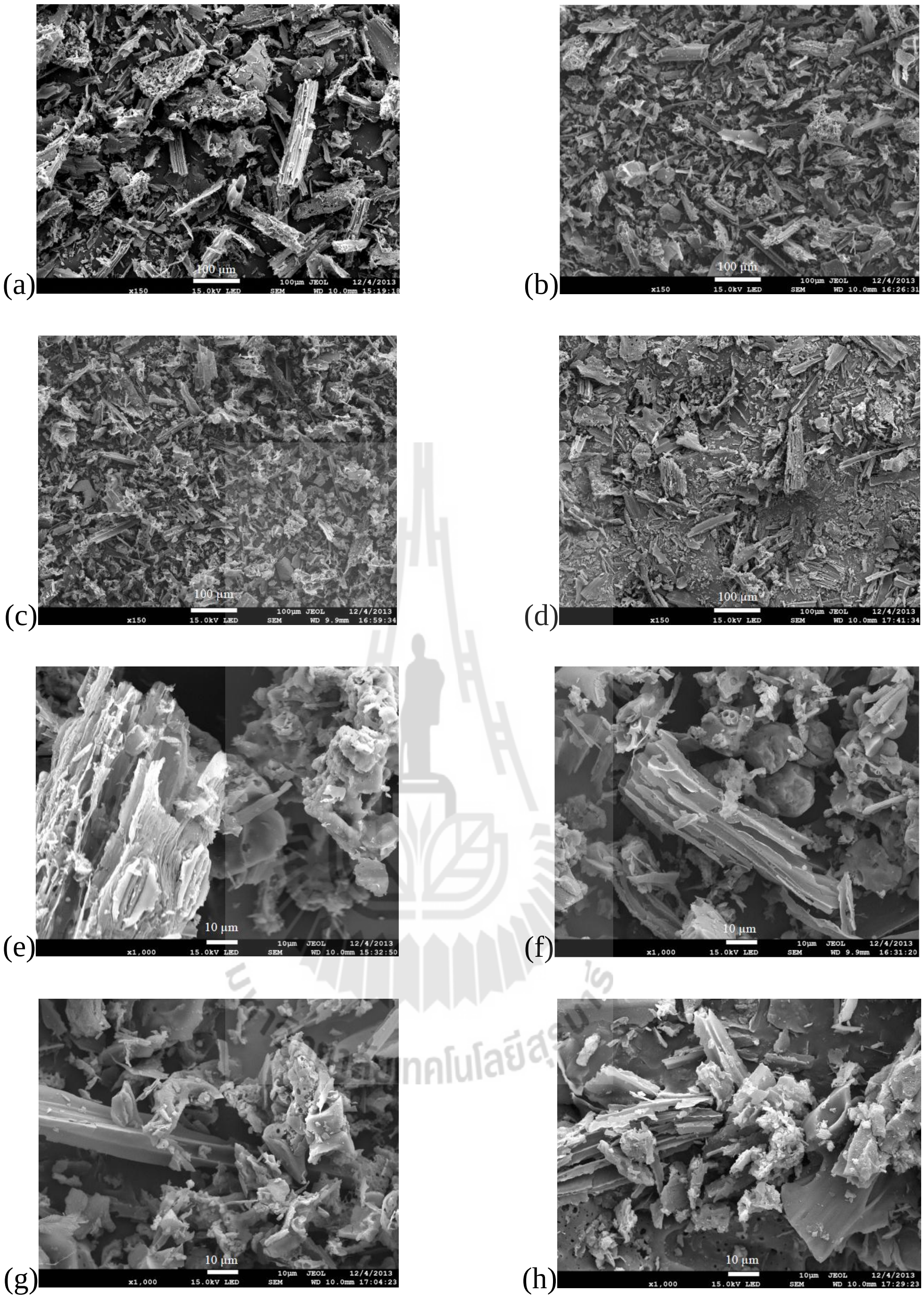

Figure 4.6 SEM imagesof (a) SCBA, (b) SCBA-NaOH-1h, (c) SCBA-NaOH-6h and (d) SCBA-hydrothermal at 150x magnification, (e) SCBA, (f) SCBA-NaOH-1h, (g) SCBA-NaOH-6h and (h) SCBA-hydrothermal at 1000x magnification. The scale bars for (a)-(d) are for the length of 100 µm and these for (e)-(h) are for the length of 10 µm.

4.3 Screening of adsorbents for the adsorption of oleic acid

Adsorption of oleic acid was initially conducted with SB, treated SBs, SCBA and treated SCBA to obtain the potential adsorbent to be investigated further. Adsorption experiments were carried out with the fixed amount of the adsorbents at 0.20 g and the concentration of oleic acid at 0.25%. The adsorption was conducted in a temperature-controlled water bath at 25 ^{o}C for 30 min with stirring provided. After that the mixture was left unstirred for 30 min to allow the particles to settle at the bottom of the flask. The clear solution was used for the determination of the unadsorbed oleic acid using the method of HPLC. The adsorption capacities for oleic acid of all adsorbents are summarized in Table 4.3. The HPLC calibration data are shown in Appendix B.

SB-H_2SO_4 has slightly higher adsorption capacity than SB which has the lowest adsorption capacity among the tested adsorbents. The adsorbents obtained from SB treated with H_2SO_4 and calcined and those from the heat treated only SBs have higher adsorption capacity compared to the nonheat treated SBs. This could be due to the higher silica content that was obtained after calcination. Among these adsorbents, SB-500 has the highest adsorption capacity. The adsorption of oleic acid occurred via hydrogen bonding of the oxygen of the carboxyl group of the acid with the hydrogen of the silanol group. The hydrogen of the carboxyl group of the acid can also form a hydrogen bond with the oxygen of the silanol group (Atia, El-Nahas, Marie and Al Mahdy, 2006, Blyholder, Adhikar and Proctor, 1995). In addition, the adsorption could occur through carboxylate ion interacting with potassium oxide (Proctor, Adhikar and Blyholder, 1995) and calcium oxide on the surface of the adsorbent.

From the adsorption results, highest adsorption capacity was obtained with SCBA-hydrothermal. Therefore, SCBA-hydrothermal was used further to study the

Table 4.3 The adsorption capacities of the studied adsorbents.

Adsorbent	Adsorption capacity (mg/g)
SB	3.3
SB-H_2SO_4	8.4
SB-H_2SO_4-400	26.9
SB-H_2SO_4-500	24.0
SB-400	25.1
SB-500	38.6
SCBA	26.8
SCBA-NaOH-1h	15.2
SCBA-NaOH-2h	18.4
SCBA-NaOH-3h	20.1
SCBA-NaOH-6h	22.7
SCBA-hydrothermal	40.2

adsorption of oleic acid. In addition, further characterization of SCBA adsorbents was also made.

4.3.1 Nitrogen adsorption-desorption analysis of SCBA adsorbents

SCBA, SCBA-NaOH-1h and SCBA-hydrothermal were subjected to N_2 adsorption-desorption analysis to obtain their textural properties. N_2 adsorption-desorption isotherms of the adsorbents are shown in Figure 4.7. According to IUPAC classification, the isotherms of the adsorbents could be assigned to be type II which is a characteristic of nonporous materials. Steep rise of N_2 intake at $P/P_0 < 0.1$ indicates the present of micropores. A hysteresis loop at $P/P_0 > 0.4$ could be from the aggregrates of particles (Rouquerol, Rouquerol and Sing, 1999), which can be seen in the SEM images in Figure 4.6. The values of the surface area and specific pore volumes are summarized in Table 4.4.

The BET surface area of SCBA after treated with 6 M NaOH for 1 h decreased from 175 m^2/g to 118 m^2/g probably from the dissolution of silica. However, when SCBA was treated with NaOH solution under hydrothermal condition, the surface area increased. This could be from the reprecipitation of the dissolved silica to form smaller silicate particles. A group of researchers reported similar experiments conducted by treating bagasse fly ash with 3 M NaOH solution at 100 °C for 72 h (Shah, Tailor and Shah, 2012). They obtained zeolitic material, mainly zeolite-P, mixed with the bagasse fly ash.

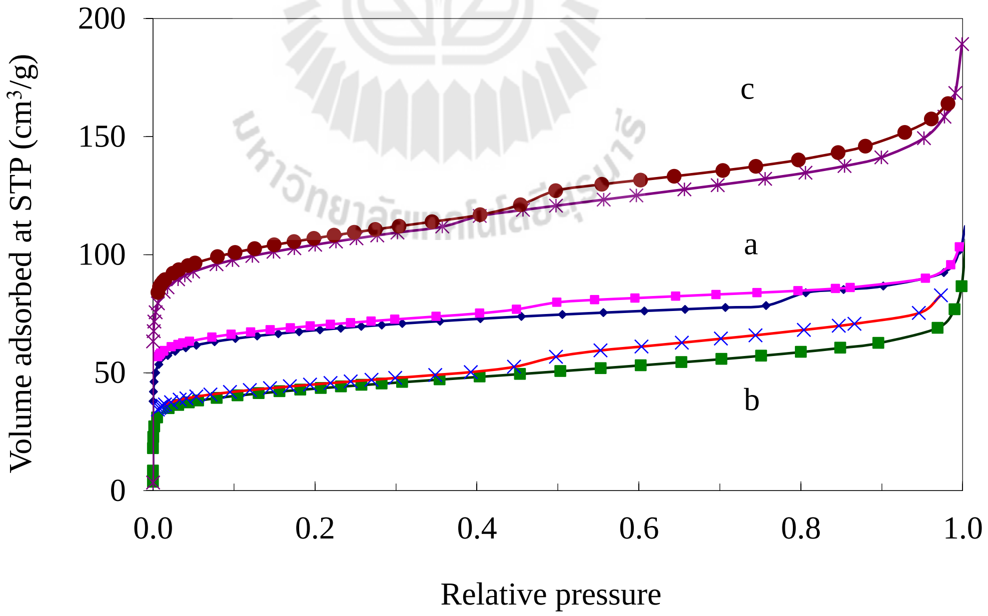

Figure 4.7 N_2 adsorption-desorption isotherms of (a) SCBA, (b) SCBA-NaOH-1h and (c) SCBA-hydrothermal. Adsorption data are shown in Appendix C.

Table 4.4 Results from N_2 adsorption-desorption analysis.

Adsorbents	BET surface area (m^2/g)	Total pore volume (cm^3/g)
SCBA	175	0.1528
SCBA-NaOH-1h	118	0.1189
SCBA-hydrothermal	264	0.2596

4.3.2 Fourier transform infrared spectroscopy analysis

Figure 4.8 presents the infrared spectra of SCBA and SCBA-hydrothermal that were examined in the range of 4000-400 cm^{-1}. FT-IR spectra of SCBA and SCBA-hydrothermal are relatively similar. A wide band about 3400-3500 cm^{-1} corresponds to symmetric and asymmetric stretching vibration of O-H group, indicating the presence of surface hydroxyl groups and physically absorbed water on the silica surface. The band at 1641 cm^{-1} is due to bending of H-OH (Frías, Villar and Savastano, 2011). The bands about 2940, 2883 and 1405 cm^{-1} are attributed to carbon residues (Frías, Villar and Savastano, 2011). The bands about 1176, 798 and 696, 472 cm^{-1} are related to Si-O-Si network (Frías, Villar and Savastano, 2011)

The FT-IR spectrum of oleic acid is shown in Figure 4.9. The band observed at 3000 cm^{-1} is the C-H stretch for an R-CH=CH-R´ group. The asymmetric C-H stretching vibration of a CH_2 groupis observed at 2930 and 2857 cm^{-1}. The band at 1709 cm^{-1} is the carbonyl stretching group. The CH_2 deformation is observed at 1460 cm^{-1} and the skeletal vibration is observed at 1284 and 954 cm^{-1} (Yates, Caldwell and Perkins, 1997).

The FT-IR spectrum of SCBA-hydrothermal after adsorption of oleic acid (SCBA-hydrothermal-oleic) shows some changes in the band pattern in the range of

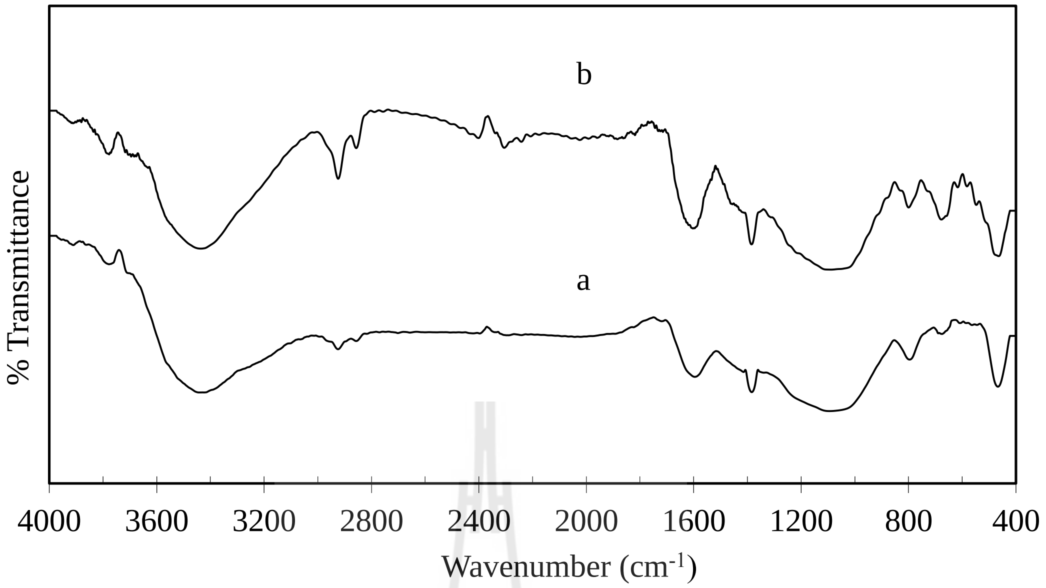

Figure 4.8 FT-IR spectraof (a) SCBA and (b) SCBA-hydrothermal.

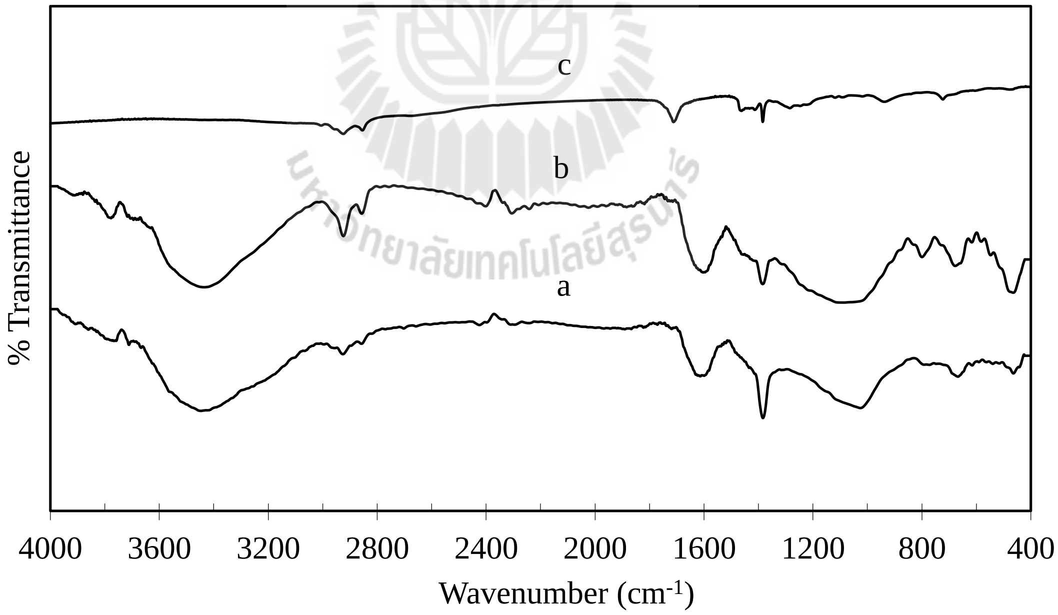

Figure 4.9 FT-IR spectra of (a) SCBA-hydrothermal, (b) SCBA-hydrothermal-oleic and (c) oleic acid.

400-900 cm^{-1} relating to the silica network, which suggests the adsorption on silica surface. The adsorption of oleic acid occurred via H-bonding of Si-O-H on the surface of silica and the carbonyl group (C=O) of oleic acid (Yates, Caldwell and Perkins, 1997). Hydrogen of the carboxylic group could also form H-bond with the OH groups on the silica surface (Blyholder, Adhikar and Proctor, 1995).

4.4 Adsorption of oleic and capric acid in isooctane

4.4.1 Adsorption of oleic acid in isooctane on SCBA-hydrothermal

SCBA-hydrothermal with the fixed weight of 0.20 g was used for the adsorption of oleic acid solutions. The concentration of oleic solution was varied in the range of 0.25-2.00%. The adsorption was carried out in a temperature-controlled water bath at 25, 35 and 45 ^{o}C for 30 min with stirring provided. After the first 30 min, the mixture was left unstirred for another 30 min before the separation of the adsorbent by filtration. The concentration of oleic acid in the solution was determined using the method of HPLC. The results are shown in Figure 4.10.

The amount of oleic acid adsorbed increased with the initial concentration of oleic acid at a constant temperature. The increase of concentration enhances the driving force to transfer oleic acid from the bulk solution to the adsorbent surface (Freitas, Mendes and Coelho, 2007).

Linear forms of Langmuir and Freundlich isotherm model were used for fitting the adsorption data at all studied temperatures and the results are shown in Table 4.5 and 4.6. Langmuir model can be examined from the plot of $1/q_e$ versus $1/C_e$ and Freundlich model can be examined from the plot of $\ln q_e$ versus $\ln C_e$.

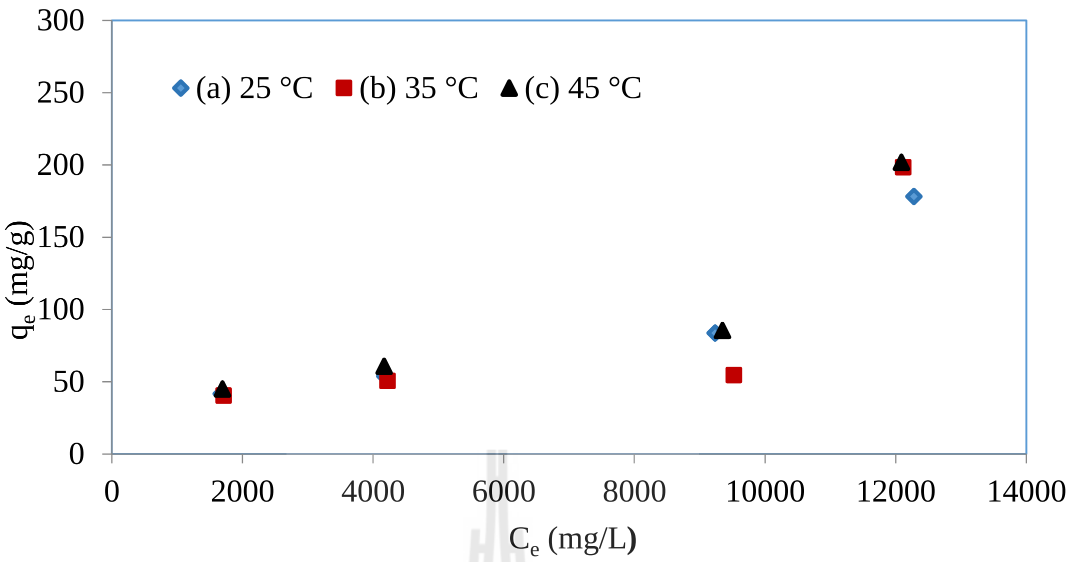

Figure 4.10 Adsorption capacities of SCBA-hydrothermal for oleic acid at various concentrations at (a) 25 °C, (b) 35 °C and (c) 45°C.

For Langmiur model the correlation coefficients (R^2) of all adsorption isotherms are >0.90. Howerver, the values of q_m and K_L at 25 and 45 °C are negative which are physically meaningless. This suggests that the Langmuir model is not appropriate model to explain the adsorption of oleic acid on SCBA-hydrothermal.

For Freundlich model, the correlation coefficients are >0.99. The values of n are about 1, indicating that the adsorption is favorable. Therefore, the adsorption of oleic acid on SCBA-hydrothermal follows the Freunlich model.

To investigate the effect of the mass of the adsorbent on the adsorption, the adsorption study was carried out using various amount of SCBA-hydrothermal with 25 mL of 0.25% oleic acid solution at 25 °C. The adsorption time was 1 h. The adsorption capacities and %removal for oleic acid are shown in Figure 4.11 and 4.12, respectively. When increased the amount of SCBA-hydrothermal from 0.05 to 0.25 g,

Table 4.5 Langmuir isotherm models, Langmuir constants and other derived parameters for the adsorption oleic acid onto SCBA-hydrothermal.

Temperature (^{o}C)	Linear equation[a]	R^2	q_m (mg/g)	K_L (L/mg)
25	y = 8.03789x - 0.00003	1.0000	-3.33×10^{4}	-3.75×10^{-6}
35	y = 6.23013x + 0.00367	0.9983	3.67×10^{3}	5.89×10^{-4}
45	y = 7.98118x - 0.00027	0.9890	-3.70×10^{3}	-3.38×10^{-5}

[a] A linear form of Langmuir model is: $\frac{1}{q_e} = \frac{1}{K_L q_m C_e} + \frac{1}{q_m}$.

Table 4.6 Freundlich isotherm models, Freundlich constants and other derived parameters for the adsorption of oleic acid onto SCBA-hydrothermal.

Temperature (^{o}C)	Linear equation[a]	R^2	n	K_F (L/g)
25	y = 1.0015x - 2.0914	1.0000	1.00	0.1235
35	y = 0.9285x - 1.6172	0.9976	1.08	0.1985
45	y = 0.9840x - 1.9504	0.9909	1.02	0.1422

[a] A linear form of Freundlich model is $\ln q_e = \ln K_F + \frac{1}{n}\ln C_e$.

the adsorption capacity and %removal increased. This trend is expected because as the adsorbent particles surrounding the oleic acid increases, more oleic acid attached to these particles (Al-Asheh, Banat and Abu-Aitah, 2003). The percentage of oleic acid removed from solutions increased from 2 to 23% with increase adsorbent dosage from 0.05 to 0.25 g.

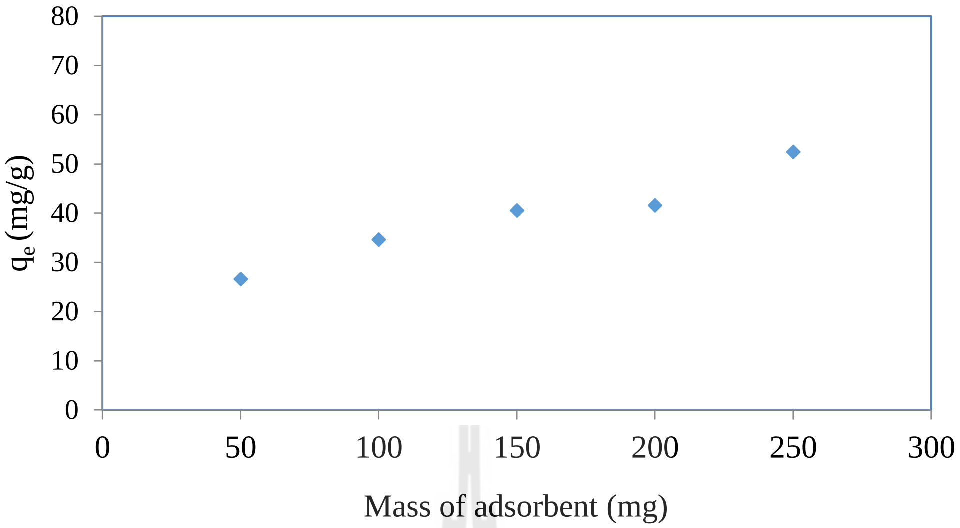

Figure 4.11 Effect of the amount of adsorbent on the adsorption capacity of oleic acid at 25°C.

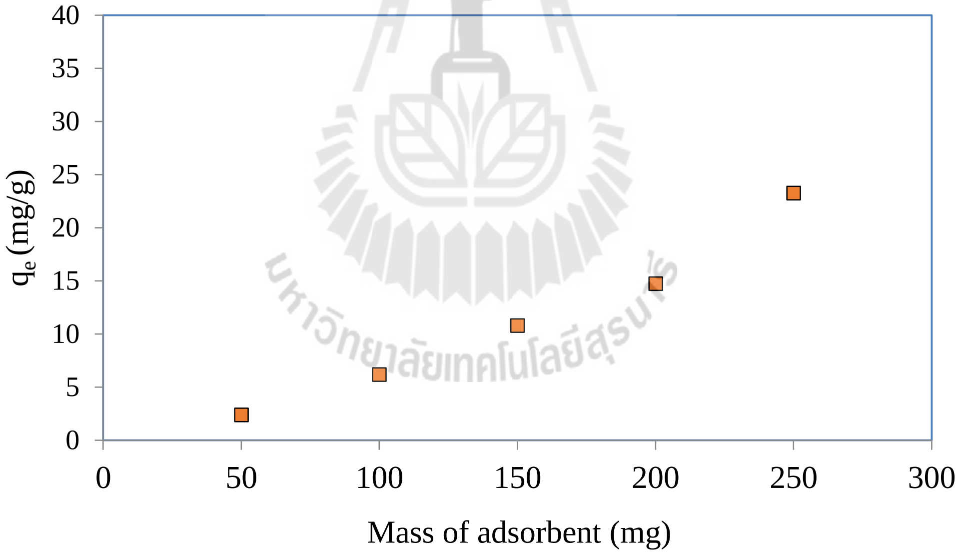

Figure 4.12 Effect of the amount of adsorbent on the %removal of oleic acid at 25 °C.

4.4.2 Adsorption of capric acid in isooctane on SCBA-hydrothermal

Capric acid or dodecanoic acid ($CH_3(CH_2)_8COOH$), a medium-chain saturated fatty acid was also used in the adsorption study with SCBA-hydrothermal to investigate the adsorption behavior of the adsorbent. To study the adsorption capacity of SCBA-hydrothermal with capric acid, the adsorption study was carried out by using 0.20 g of SCBA-hydrothermal and various concentrations of capric acid in the range of 0.05-2.00%. The adsorption was carried out in a temperature-controlled water bath at 25 °C for 30 min with stirring provided. After the first 30 min, the mixture was let unstirred for another 30 min. The clear solution was used for the determination of unadsorbed capric acid using the titration method. The adsorption capacities for capric acid are shown in Figure 4.13.

The adsorption capacity rises steeply at low acid concentrations and reaches to a horizontal plateau at higher concentrations. This suggests the formation of a monolayer of capric acid on the SCBA-hydrothermal (Bayrak, 2006). The adsorption capacity of the adsorbent for capric acid is higher than that for oleic acid. The smaller capric acid structure could hinder the adsorption sites to a lesser extent compared to oleic acid.

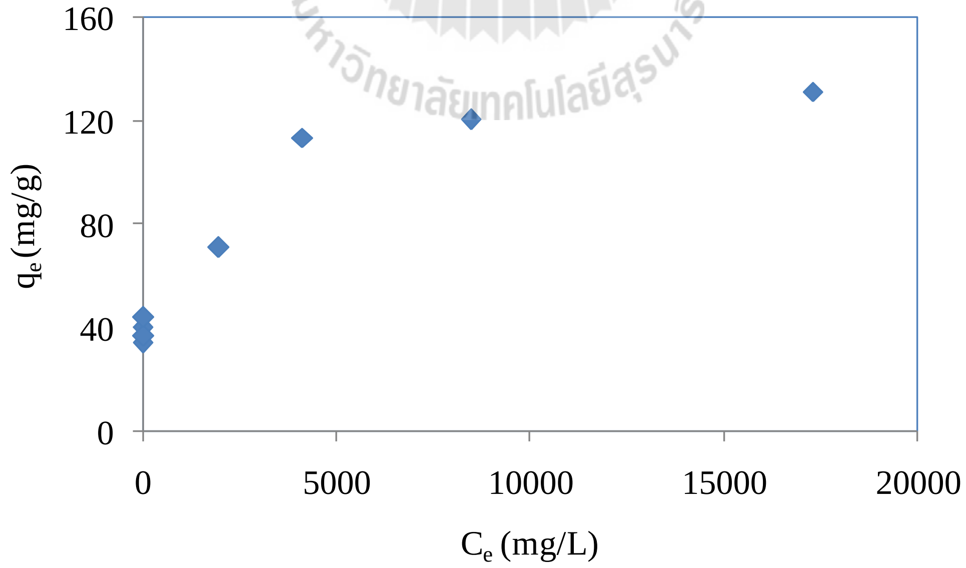

Figure 4.13 Adsorption isotherm of capric acid on SCBA-hydrothermal.

Table 4.7 The dimensionless constant separation factors for the adsorption of capric acid onto SCBA-hydrothermal at various concentration of capric acid at 25 ^{o}C.

C_o (%)	0.05	0.07	0.10	0.15	0.25	0.50	1.00	2.00
R_L	0.41	0.38	0.29	0.23	0.14	0.07	0.04	0.02

To examine the applicability of Langmuir isotherm with the adsorption data, a plot of C_e/q_e versus C_e shown in Appendix D was made. The regression equation is y = 0.0076x + 3.0898 with R^2 = 0.9908. The derived q_m and K_L are 131.58 mg/g and 0.0025 L/mg, respectively. In addition, fitting the adsorption data with Freundlich isotherm was also made by examining a plot of $\ln q_e$ versus $\ln C_e$. The obtained regression equation is y = 0.1677x + 3.2185 with R^2 = 0.9539. The values of n and K_F are 5.96 and 24.99 ($mg^{1-1/n}.L^{1/n}/g$), respectively. Langmuir isotherm seems to apply well with the adsorption data. Further investigation of the dimensionless constant separation factor, R_L, for all concentrations of the acid revealed that the values of R_L are in the range of 0-1 as shown in Table 4.7. This indicates that the adsorption is favorable.

With the available data, the Gibbs free energy change (ΔG) could be estimated using equation (6). The calculated value of ΔG is -15.0 KJ/mol. The negative value of ΔG indicates that the adsorption is spontaneous.

4.5 Adsorption of oleic and capric acid in soybean oil

SCBA-hydrothermal was used in the adsorption of oleic or capric acid in soy bean oil samples. The adsorption study was carried out by using 0.20 g of adsorbent mixed in 25 mL solution of 0.50 and 1.00% oleic or capric acid in soybean oil at 25 ^{o}C.

Table 4.8 Adsorption of oleic acid or capric acid in soy bean oil at 25 ^{o}C.

Acid	Concentration (%)	Adsorption capacities(mg/g)	%Removal
oleic acid	0.50	11.58	1.45
	1.00	62.30	4.72
capric acid	0.50	78.84	13.66
	1.00	90.30	8.66

The solution was stirred for 30 min in a temperature-controlled water bath at 25^{o}C and then left unstirred for 30 min. After that the adsorbent was removed by centrifugation. The unadsorbed oleic and capric acid were determined using the method of an American Oil Chemists' Society (AOCS Ca 5a 40).The results are shown Table 4.8. The adsorption capacities of oleic and capric acid in soybean oil are lower than those in isooctane. This could be from the competitive adsorption of the investigated acids and triacylglycerol which could also be adsorbed on the adsorbent. Mechanism for triacylglycerol adsorption on the adsorbent is similar to that of the acids as reported in the literature (Yates et al., 1997).

4.6 References

Al-Asheh, S., Banat, F. and Abu-Aitah, L. (2003). Adsorption of phenol using different types of activated Bentonites. **Separation and Purification Technology**. 33: 1-10.

Atial, A. A., El-Naha, A. M., Mari, A. M. and Al Mahdy, L. D. (2006) Adsorption of oleic acid on silica gel derived from rice ash hulls: Experimental and theoretical studies. **Adsorption Science and Technology**. 24(9): 797-814.

Bayrak, Y. (2006) Application of Langmuir isotherm to saturated fatty acid adsorption. **Microporous and Mesoporous Materials**. 87: 203-206.

Blyholder, G., Adhikar, C. and Proctor, A. (1995) Structure and orientation of oleic acid adsorbed onto silica gel. **Colloids and Surfaces A: Physicochemical and Engineering Aspects**. 105: 151-158.

Chen, W. H., Tu, Y. J. and Sheen, H. K. (2011) Disruption of sugarcane bagasse lignocellulosic structure by means of dilute sulfuric acid pretreatment with microwave-assisted heating. **Applied Energy**. 88: 2726-2734.

Freire, M. N. and Holanda, J. N. F. (2006) Characterization of avian eggshell waste aiming its use in a ceramic wall tile paste. **Journal of the Brazilian Ceramic Society**. 52: 240-244.

Freitas, A. F., Mendes M. F. and Coelho G. L. V. (2007) Thermodynamic study of fatty acids adsorption on different adsorbents. **The Journal of Chemical Thermodynamics**. 39: 1027-1037.

Frías, M., Villar, E. and Savastano, H. (2011) Brazilian sugar cane bagasse ashes from the cogeneration industry as active pozzolans for cement manufacture. **Cement and Concrete Composites**. 33: 490-496

Gastaldi, D., Boccaleri, E., Canonico, F. and Bianchi, M. (2007) The use of Raman spectroscopy as a versatile characterization tool for calcium sulphoaluminate cements: a compositional and hydration study. **Journal of Materials Science**. 42: 8426-8432.

Le Blond, J. S., Horwell, C. J., Williamson, B. J. and Oppenheimer, C. (2010) Generation of crystalline silica from sugarcane burning. **Journal of Environmental Monitoring**. 12: 1459-1470.

Paya´, J., Monzo´, J., Borrachero, MV.,Dı´az-Pinzo´n, L. and M Ordo´n˜ez, LM. (2002) Sugar-cane bagasse ash (SCBA): studies on its properties for reusing in concrete production. **Journal of Chemical Technology and Biotechnology**. 77: 321-325.

Pereira, P. H. F., Voorwald, H. C. J., Cioffi, M. O. H., Mulinari, D. R., Da Luz, S. M. and Da Silva, M. L. C. P. (2011) Sugarcane bagasse pulping and bleaching: thermal and chemical characterization. **BioResources**. 6(3): 2471-2482.

Proctor, A., Adhikar, C. and Blyholder, G. (1995) Mode of oleic acid adsorption on rice hull ash cristobalite. **Journal of the American Oil Chemists' Society**. 72(3): 331-335.

Rouquerol, F.; Rouquerol, J.; Sing, K. **Adsorption by Powders and Porous Solids: Principles, Methodology and Applications**; Academic Press, California, 1999; pp 440-441.

Shan, B., Mistry, C. and Shan, A. (2013) Seizure modeling of Pb (II) and Cd (II) from aqueous solution by chemically modified sugarcane bagasse fly ash: isotherms, kinetics, and column study. **Environmental Science and Pollution Research**. 20(4): 2193-2209.

Shah, B., Tailor, R. and Shah, A. (2012) Equilibrium, kinetics, and breakthrough curve of phenol sorption on zeolitic material derived from BFA. **Journal of Dispersion Science and Technology**. 33: 41-51.

Teixeira, S. R., Souza, A. E. Santos, G. T. A. and Peña, A. F. V. (2008) Sugarcane bagasse ash as a potential quartz replacement in red ceramic. **Journal of the American Ceramic Society**. 91: 1883-1887.

Umeda, J., Kondoh, K. and Michiura, Y. (2007) Process parameters optimization in preparing high-purity amorphous silica originated from rice husks. **Materials Transactions**. 48(12): 3095-3100.

Yates, R. A., Caldwell, J. D. and Perkins, E. G. (1997). Diffuse reflectance fourier transform infrared spectroscopy of triacylglycerol and oleic acid adsorption on synthetic magnesium silicate. **Journal of the American Oil Chemists' Society**. 74 (3): 289-292.

CHAPTER V

CONCLUSION

In this research, sugarcane bagasse (SB) and sugarcane bagasse ash (SCBA) were subjected to simple treatment methods using solutions of sulfuric acid, sodium hydroxide and heat to produce adsorbents for the adsorption of oleic acid. Among the derived adsorbents, hydrothermally treated SCBA has the highest adsorption capacity for oleic acid. The adsorption of oleic acid follows Freundlich isotherm model, while the adsorption of capric acid follows the Langmuir isotherm model.

Silica contained in SCBA is assumed to play a major role in the adsorption of oleic and capric acid. Hydrothermal treatment of SCBA leads to smaller particle size and higher surface area which contribute to higher adsorption capacity of the adsorbent.

To investigate the applicability of the hydrothermally treated SCBA, it was used in the adsorption of oleic and capric acid in soy bean oil. The adsorption capacities of the adsorbent were lower than those of the adsorption conducted in isooctane as a solvent. Lower adsorption capacities could be from the competitive adsorption of triacylglycerol on the adsorbent. Therefore, it is suggested that to remove more amount of the acid from the oil, higher amount of the adsorbent should be used.

SCBA-hydrothermal is a good candidate to be used as the adsorbent for the removal of free fatty acids in oil samples. SCBA itself is considered as a waste from boilers, therefore making use of SCBA should be beneficial to the environment. In addition, the treatment condition to produce the adsorbent is simple and mild and requires only the use of low cost chemicals. Therefore, it could be economical to produce a large amount of the adsorbent for the future use.

APPENDICES

APPENDIX A

SEM IMAGE OF ADSORBENTS

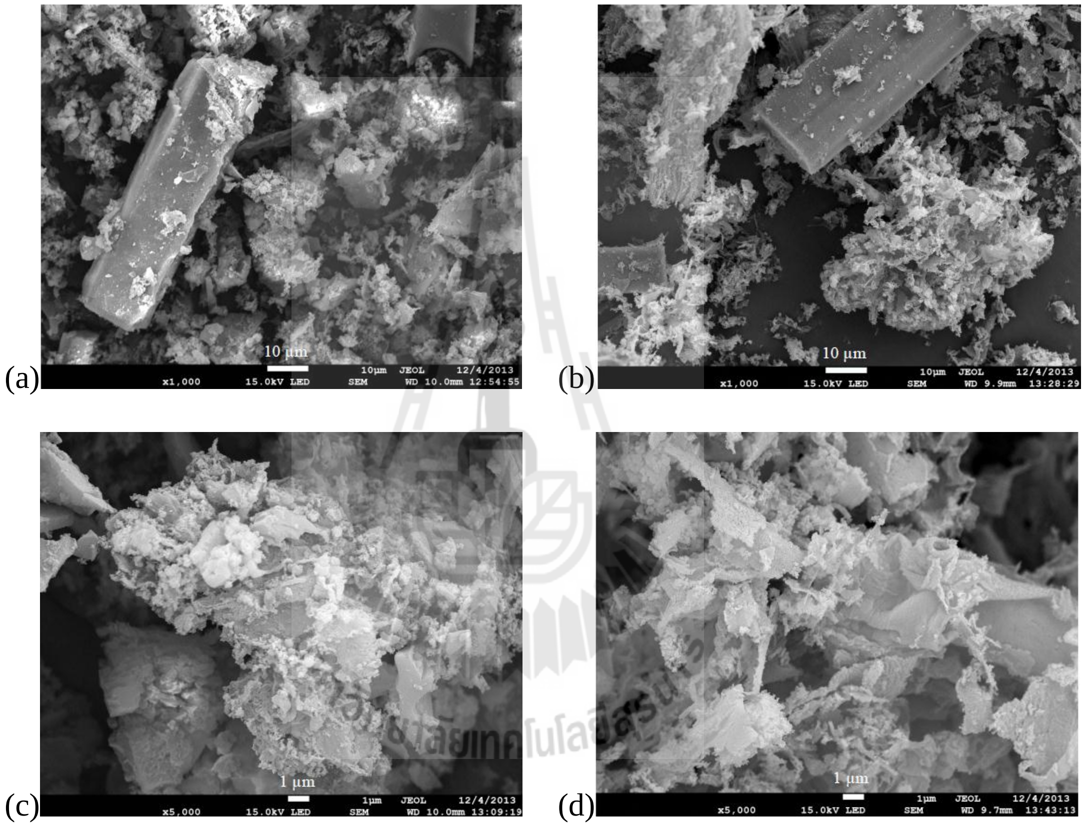

Figure A.1 SEM images of (a) SB-H_2SO_4-500 and (b) SB-500 with a magnitude of 1000x, (c) SB-H_2SO_4-500 and (d) SB-500 with a magnitude of 5000x.

APPENDIX B

DETERMINATION OF OLEIC ACID BY HPLC

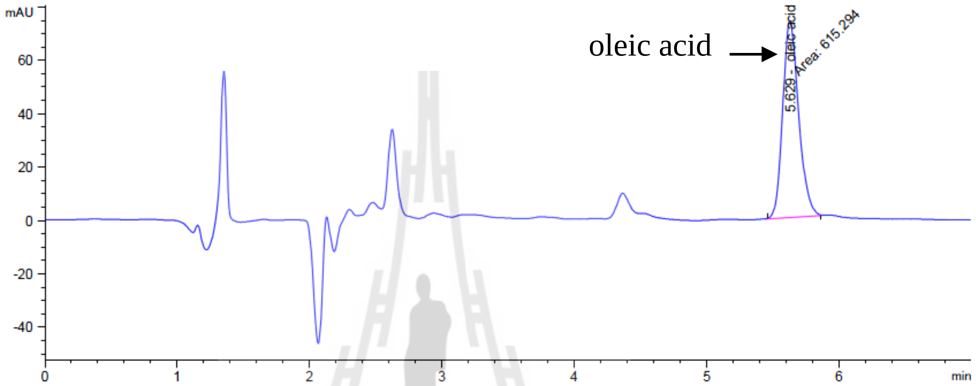

Figure B.1 A chromatogram of 20 ppm of oleic acid. A column used in the analysis was Hypersil ODS C-18. A mobile phase was acetonitrile mixed with 0.4% acetic acid with the volume ratio of 90:10. A detector was a UV spectrometer recording absorbance at 195 nm.

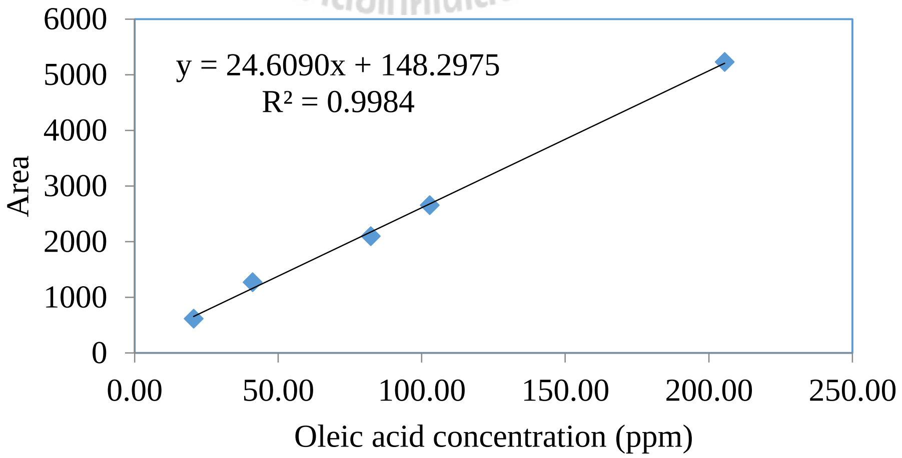

Figure B.2 A calibration curve for the determination of oleic acid for the adsorption conducted at 25 ^{o}C.

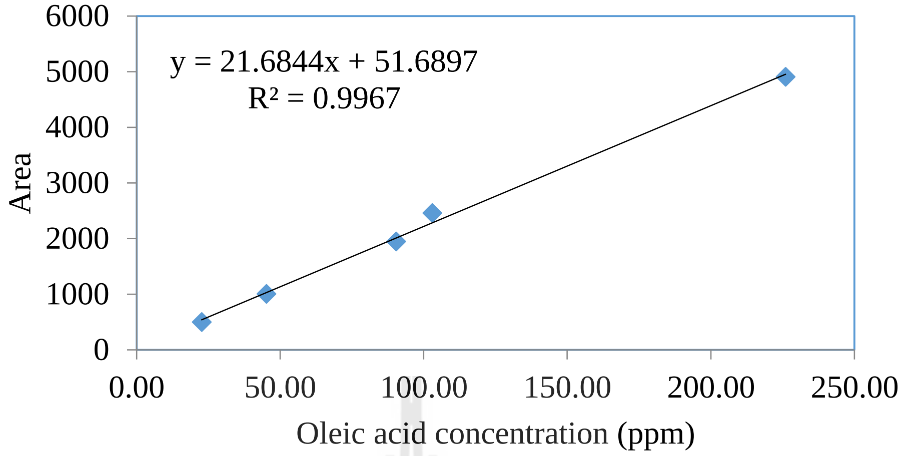

Figure B.3 A calibration curve for the determination of oleic acid for the adsorption conducted at 35 °C.

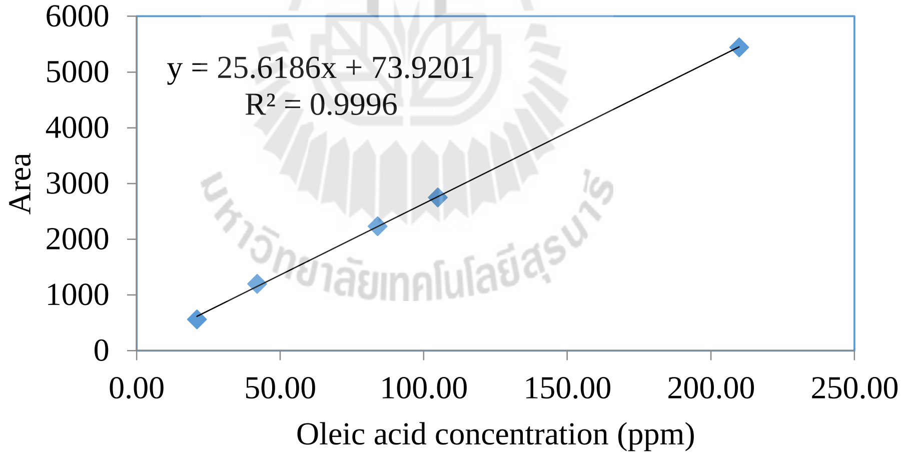

Figure B.4 A calibration curve for the determination of oleic acid for the adsorption conducted at 45 °C.

APPENDIX C

DATA FROM N_2 ADSORPTION-DESORPTION

Table C.1 N_2 adsorption-desorption of SCBA.

Relative pressure (P/P_o)	Volume adsorbed (cm^3/g STD)	Relative pressure (P/P_o)	Volume desorbed (cm^3/g STD)
-2.38000E-19	3.300	0.99610	103.150
-2.38000E-19	7.112	0.98510	95.646
-0.000082	10.947	0.95400	89.944
-0.000082	14.786	0.86110	86.009
-0.000082	18.632	0.84300	85.561
-0.000082	22.462	0.79670	84.655
-0.000082	26.296	0.74600	83.832
-0.000082	30.141	0.69540	83.082
-0.000041	33.980	0.64530	82.322
0.000029	37.816	0.59530	81.551
0.000357	42.012	0.54520	80.794
0.001180	46.088	0.49870	79.716
0.003140	49.897	0.44870	76.792
0.006930	53.426	0.40330	75.100
0.018000	57.245	0.34960	73.765
0.027400	59.041	0.29850	72.536
0.040400	60.508	0.26940	71.799
0.053200	61.630	0.24400	71.124
0.075700	63.084	0.21900	70.432
0.101700	64.409	0.19420	69.705
0.128400	65.525	0.16950	68.940

Table C.1 N_2 adsorption-desorption of SCBA. (Continued)

Relative pressure (P/P_o)	Volume adsorbed (cm^3/g STD)
0.154700	66.478
0.180300	67.354
0.206200	68.122
0.231600	68.841
0.256900	69.533
0.282400	70.164
0.307500	70.767
0.354300	71.793
0.404200	72.807
0.454900	73.752
0.505600	74.602
0.556200	75.392
0.606800	76.133
0.656800	76.840
0.706900	77.563
0.757200	78.349

Relative pressure (P/P_o)	Volume desorbed (cm^3/g STD)
0.14480	68.111
0.12040	67.204
0.09630	66.199
0.07260	65.026

Table C.2 N_2 adsorption-desorption of SCBA-NaOH-1h.

Relative pressure (P/P_o)	Volume adsorbed (cm^3/g STD)	Relative pressure (P/P_o)	Volume desorbed (cm^3/g STD)
2.8544E-05	3.735	0.9729	82.768
-3.1236E-19	8.489	0.9457	75.228
-4.0788E-05	13.244	0.8663	70.726
-3.1245E-19	17.990	0.8469	69.838
0.000274	22.682	0.8035	68.129
0.001549	27.125	0.7438	65.867
0.005145	30.959	0.7013	64.400
0.019522	34.869	0.6531	62.740
0.031301	36.288	0.6031	61.083
0.044318	37.323	0.5527	59.442
0.055690	38.147	0.4976	56.780
0.078724	39.267	0.4459	52.470
0.104200	40.308	0.3923	50.269
0.130400	41.204	0.3484	49.059
0.156000	42.018	0.2990	47.756
0.181700	42.755	0.2697	46.981
0.207100	43.442	0.2440	46.291
0.232200	44.104	0.2189	45.606
0.257400	44.745	0.1939	44.910
0.282500	45.368	0.1690	44.191
0.307700	45.992	0.1442	43.434
0.353900	47.097	0.1195	42.632
0.403200	48.262	0.0950	41.758
0.453400	49.447	0.0709	40.754
0.503000	50.651	0.0533	39.876
0.552800	51.875	0.0412	39.137
0.602500	53.128	0.0327	38.513

Table C.2 N_2 adsorption-desorption of SCBA-NaOH-1h. (Continued)

Relative pressure (P/P_o)	Volume adsorbed (cm^3/g STD)	Relative pressure (P/P_o)	Volume desorbed (cm^3/g STD)
0.652400	54.427	0.0222	37.520
0.702100	55.761	0.0146	36.501
0.751200	57.185	0.0120	36.028
0.800100	58.746	0.0096	35.514
0.848600	60.485	0.0076	34.981
0.896000	62.526	0.0058	34.374
0.969000	68.958		
0.989900	76.782		
0.998800	86.599		
1.003900	106.520		

Table C.3 N_2 adsorption-desorption of SCBA-hydrothermal.

Relative pressure (P/P_o)	Volume adsorbed $(cm^3/g\ STD)$	Relative pressure (P/P_o)	Volume desorbed $(cm^3/g\ STD)$
-2.37E-19	3.3977	0.9818	163.990
-4.05E-05	7.373	0.9613	157.420
-4.05E-05	11.34	0.9282	151.780
-0.00012	15.324	0.8798	145.920
-0.00016	19.311	0.8460	143.250
-0.00020	23.291	0.7970	140.110
-0.00020	27.269	0.7444	137.440
-0.00024	31.272	0.7037	135.640
-0.00028	35.278	0.6436	133.210
-0.00028	39.284	0.6018	131.610
-0.00024	43.288	0.5540	129.790
-0.00028	47.302	0.4970	127.050
-0.00028	51.309	0.4537	121.150
-0.00020	55.302	0.4038	116.870
-0.00008	59.270	0.3446	113.960
0.00007	63.221	0.3038	112.070
0.00064	67.506	0.2745	110.690
0.00158	71.665	0.2485	109.430
0.00329	75.562	0.2233	108.170
0.00605	79.345	0.1985	106.880
0.01307	84.282	0.1740	105.520
0.01783	86.086	0.1494	104.110
0.03078	89.561	0.1252	102.590
0.03926	91.172	0.1013	100.920
0.04952	92.746	0.0794	99.165
0.07812	95.919	0.0518	96.411
0.09823	97.652	0.0431	95.318

Table C.3 N$_2$ adsorption-desorption of SCBA-hydrothermal. (Continued)

Relative pressure (P/P$_o$)	Volume adsorbed (cm^3/g STD)
0.12250	99.468
0.14850	101.160
0.17430	102.730
0.20010	104.190
0.22560	105.570
0.25120	106.880
0.27670	108.140
0.30170	109.370
0.35720	111.840
0.40350	116.340
0.45680	118.900
0.49740	120.700
0.55660	123.300
0.59690	125.050
0.65630	127.650
0.69720	129.440
0.75580	132.130
0.80570	134.650
0.85410	137.540
0.89940	141.160
0.95200	149.330
0.97740	158.440
0.99080	168.410
0.99920	189.200

Relative pressure (P/P$_o$)	Volume desorbed (cm^3/g STD)
0.0315	93.526
0.0244	92.147
0.0145	89.445
0.0121	88.578
0.0097	87.527
0.0078	86.449
0.0059	83.970

APPENDIX D

LANGMUIR AND FREUNDLICH ISOTHERM FITTING FOR THE ADSORPTION OF CAPRIC ACID ON SCBA-HYDROTHERMAL

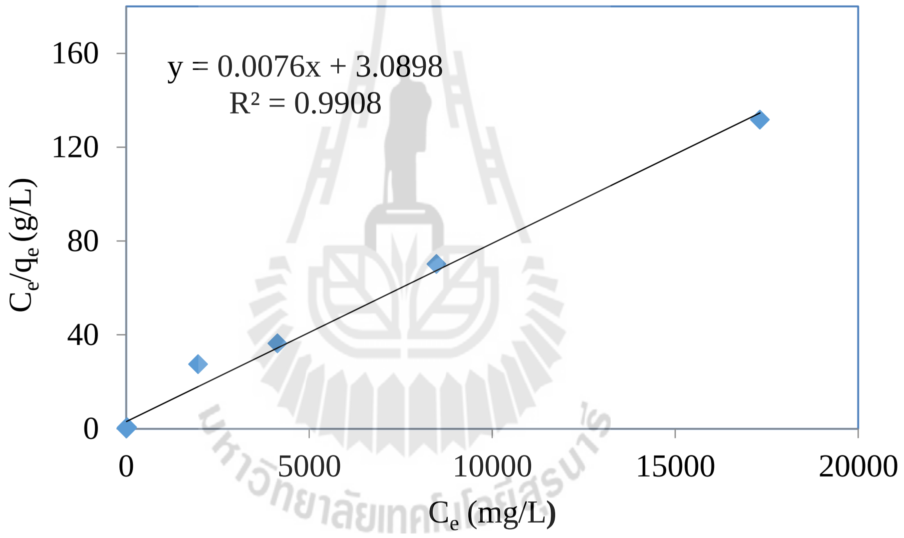

Figure D.1 The linear Langmuir isotherm fitting for capric acid adsorption in isooctane onto SCBA-hydrothermal at 25 °C.

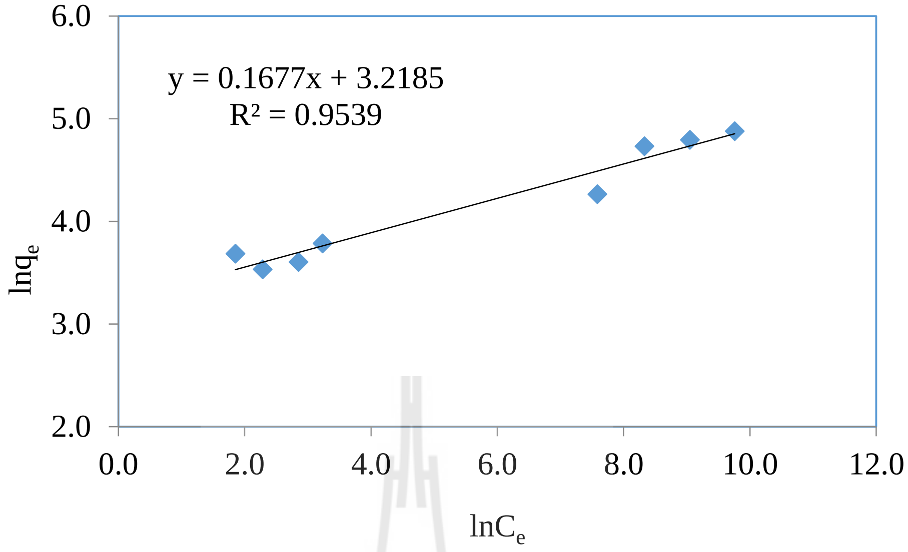

Figure D.2 The linear Freundlich isotherm fitting for capric acid adsorption in isooctane onto SCBA-hydrothermal at 25 °C.

CURRICULUM VITAE

Name	Miss Wimolmas Siriwanitch
Date of Birth	April 10th, 1968
Place of Birth	Burirum, Thailand

Education

1988-1991	B.Sc. (Chemistry), Chiangmai University
2011-Present	M.Sc. student (Chemistry), Suranaree University of Technology, Nakhon Ratchasima, Thailand

Position and Place of Work

1991 - 1993	Quality Assurance (Q.A.), Strongpack Co., Ltd
1994 - 1998	Medical Scientist, Medical Science Center, Ministry of Public Health, Thailand
2002 - present	Medical Scientist, Regional Medical Science Center 9, Nakhon Ratchasima, Ministry of Public Health, Thailand